



**HAL**  
open science

## Comprehensive and Comparative Transcriptional Profiling of the Cell Wall Stress Response in *Bacillus subtilis*

Qian Zhang, Charlene Cornilleau, Raphael R Müller, Doreen Meier, Pierre Flores, Cyprien Guérin, Diana Wolf, Vincent Fromion, Rut Carballido-Lopez, Thorsten Mascher

► **To cite this version:**

Qian Zhang, Charlene Cornilleau, Raphael R Müller, Doreen Meier, Pierre Flores, et al.. Comprehensive and Comparative Transcriptional Profiling of the Cell Wall Stress Response in *Bacillus subtilis*. 2023. hal-04314056

**HAL Id: hal-04314056**

**<https://hal.science/hal-04314056>**

Preprint submitted on 29 Nov 2023

**HAL** is a multi-disciplinary open access archive for the deposit and dissemination of scientific research documents, whether they are published or not. The documents may come from teaching and research institutions in France or abroad, or from public or private research centers.

L'archive ouverte pluridisciplinaire **HAL**, est destinée au dépôt et à la diffusion de documents scientifiques de niveau recherche, publiés ou non, émanant des établissements d'enseignement et de recherche français ou étrangers, des laboratoires publics ou privés.

1  
2  
3  
4  
5  
6  
7  
8  
9  
10  
11  
12  
13  
14  
15  
16  
17  
18  
19  
20  
21  
22

# Comprehensive and Comparative Transcriptional Profiling of the Cell Wall Stress Response in *Bacillus subtilis*

Qian Zhang<sup>1#</sup>, Charlene Cornilleau<sup>2#</sup>, Raphael R. Müller<sup>3</sup>, Doreen Meier<sup>4</sup>, Pierre Flores<sup>2</sup>, Cyprien Guérin<sup>5</sup>, Diana Wolf<sup>1</sup>, Vincent Fromion<sup>2</sup>, Rut Carballido-Lopez<sup>2§</sup>,  
and Thorsten Mascher<sup>1§</sup>

<sup>1</sup> Technische Universität (TU) Dresden, General Microbiology, Germany

<sup>2</sup> MICALIS Institute, INRAE, AgroParisTech, Université Paris-Saclay, 78350 Jouy-en-Josas, France

<sup>3</sup> Bioinformatics and Systems Biology, Justus-Liebig-Universität, Gießen, Germany

<sup>4</sup> SYNMIKRO and Philipps-Universität Marburg, Germany

<sup>5</sup> MaIAGE, INRAE, Université Paris-Saclay, 78350 Jouy-en-Josas, France.

# These two authors contributed equally to this work

§ Authors for correspondence:

[thorsten.mascher@tu-dresden.de](mailto:thorsten.mascher@tu-dresden.de), [rut.carballido-lopez@inrae.fr](mailto:rut.carballido-lopez@inrae.fr)

## 23 **Abstract**

24 The bacterial cell wall (CW) is an essential protective barrier and the frontline of cellular interactions  
25 with the environment and also a target for numerous antimicrobial agents. Accordingly, its integrity  
26 and homeostasis are closely monitored and rapid adaptive responses by transcriptional  
27 reprogramming induce appropriate counter-measures against perturbations. Here, we report a  
28 comprehensive and comparative transcriptional profiling of the primary cell envelope stress responses  
29 (CESR), based on combining RNAseq and high-resolution tiling array studies of the Gram-positive  
30 model bacterium *Bacillus subtilis* exposed to a range of antimicrobial compounds that interfere with  
31 cytoplasmic, membrane-coupled or extracellular steps of peptidoglycan (PG) biosynthesis. It revealed  
32 the complexity of the CESR of *B. subtilis* and unraveled the contribution of extracytoplasmic function  
33 sigma factors (ECFs) and two-component signal transduction systems (TCSs) to protect the cell  
34 envelope. While membrane-anchored steps are tightly controlled, early cytoplasmic and late  
35 extracellular steps of PG biosynthesis are hardly monitored at all. The ECF  $\sigma^W$  and particularly  
36  $\sigma^M$  provide a general CESR, while  $\sigma^V$  is almost exclusively induced by lysozyme, against which it provides  
37 specific resistance. Remarkably,  $\sigma^X$  was slightly repressed by most antibiotics, pointing towards a role  
38 in envelope homeostasis rather than CESR. It shares this role with the WalRK TCS, which balances CW  
39 growth with controlled autolysis. In contrast, all remaining TCSs are envelope stress-inducible systems.  
40 LiaRS is induced by a wide range of PG synthesis inhibitors, while the three paralogous systems BceAB,  
41 PsdRS and ApeRS are more compound-specific detoxification modules. Induction of the CsrRS TCS by  
42 all antibiotics interfering with membrane-anchored steps of PG biosynthesis points towards a  
43 physiological link between CESR and secretion stress. Based on the expression signatures, a suite of  
44 CESR-specific *B. subtilis* whole cell biosensors were developed and carefully evaluated. This is the first  
45 comprehensive transcriptomic study focusing exclusively on the primary effects of envelope  
46 perturbances that shall provide a reference point for future studies on Gram-positive CESR.

47

## 48 Introduction

49  
50 The bacterial cell envelope separates and protects the cell from its environment. It serves as a  
51 molecular sieve, a diffusion barrier, and a communication interface and counteracts the high internal  
52 osmotic pressure [1, 2]. In Gram-positive bacteria, it consists of the cytoplasmic membrane surrounded  
53 by a thick CW, primarily composed of two biopolymers, the peptidoglycan (PG) and the anionic wall  
54 teichoic acids. PG forms a three-dimensional network that maintains cell shape and provides physical  
55 integrity by counteracting the very high internal osmotic pressure of bacterial cells.

56  
57 **The bacterial cell wall as shield and target.** PG is made of glycan chains of alternating N-acetyl-  
58 glucosamine (GlcNAc) and N-acetyl-muramic acid (MurNAc), cross-linked by stem peptides linked to  
59 MurNAc and synthesized as pentapeptides. It is assembled in three major steps that are confined to  
60 different cellular compartments (Fig. 1): (i) the cytoplasmic assembly of soluble UDP-GlcNAc and UDP-  
61 MurNAc-pentapeptide, (ii) the membrane-associated formation of the lipid II intermediate and its  
62 translocation across the cytoplasmic membrane, referred to as the lipid II-cycle, and (iii) the  
63 incorporation and crosslinking of the GlcNAc-MurNAc-pentapeptide building block into the established  
64 PG network by transglycosylation (TG) and transpeptidation (TP) reactions [3]. After releasing the  
65 building blocks, the lipid carrier (undecaprenyl phosphate) flips back to the inner leaflet of the cell  
66 membrane and is then recycled for the next round of translocation (Fig. 1). Because of its essential  
67 function, the CW represents an attractive target for antimicrobial compounds, especially since the PG  
68 layer is a uniquely bacterial structure not found in eukaryotes. Thus, PG biosynthesis inhibitors, such  
69 as the  $\beta$ -lactams, display low target-related side effects and are still the most widely used antibacterial  
70 drugs worldwide [4]. Basically every step of the essential PG biosynthesis pathway is targeted by  
71 antibiotics [5] (Fig. 1). Fosfomycin and D-cycloserine are inhibitors of the cytoplasmic steps of  
72 precursor biosynthesis. Fosfomycin blocks the first committed step, the formation of UDP-MurNAc  
73 from UDP-GlcNAc by inhibiting the catalytic enzyme MurA [6]. D-cycloserine inhibits both the D-alanine  
74 racemase Alr and the D-Ala-D-Ala ligase DdlB that produce UDP-MurNAc-pentapeptide [7-9]. A  
75 plethora of antibiotics interfere with the membrane-anchored steps of PG biosynthesis: tunicamycin  
76 at high concentrations ( $>10 \mu\text{g/ml}$ ) blocks MraY activity in addition to the target of surface  
77 glycopolymers, thereby inhibiting the formation of lipid I (MurNAc-pentapeptide-UPP) from UDP-  
78 MurNAc-pentapeptide [10-14], while bacitracin binds to undecaprenyl pyrophosphate, thereby  
79 preventing its dephosphorylation and hence recycling of the lipid carrier [15-17]. Vancomycin is a  
80 glycopeptide antibiotic that blocks glycan polymerization and cross-linking by binding to the D-alanyl-  
81 D-alanine dipeptide terminus of newly externalized lipid II [18]. Finally, moenomycin inhibits the TG  
82 reaction of PBPs [19, 20], while the  $\beta$ -lactams (e.g. Penicillin G) interfere with their TP reaction [21].

83 Lastly, lysozyme is an enzyme that kills bacteria by hydrolyzing the 1,4- $\beta$ -link between MurNAc and  
84 GlcNAc residues in the PG [22].

85

86 **Protecting the wall: Cell envelope stress response (CESR) in *Bacillus subtilis*.** Because of its vital role  
87 and numerous potential threats, the integrity of the cell envelope is closely monitored.  
88 Countermeasures, e.g. against antibiotic action, can then be implemented to cope with stress before  
89 irreversible CW damage can occur. Collectively, these measures are termed the cell envelope stress  
90 response (CESR). In the past 25 years, the underlying regulatory network has been extensively studied  
91 in the Gram-positive model organism *B. subtilis* (summarized in [23, 24]). At least eight regulatory  
92 systems from two major signaling principles, extracytoplasmic function sigma factors (ECFs) and two-  
93 component signal transduction systems (TCSs), are involved in mediating the CESR in this organism.  
94 Four of the seven ECFs have been directly linked to counteracting stress or damage caused by CW  
95 antibiotics, of which  $\sigma^W$  and  $\sigma^M$  play a predominant role in providing a more general resistance against  
96 cell envelope damage, while  $\sigma^X$  and  $\sigma^V$  are specific for membrane perturbations or lysozyme challenge,  
97 respectively [25].  $\sigma^W$  controls a large ‘antibiosis’ regulon, with a significant number of its 60-90 target  
98 genes encoding functions implicated in antibiotic resistance. Accordingly, a *sigW* mutant is more  
99 sensitive to fosfomycin, pore-forming lantibiotics (such as nisin) and a number of antimicrobial  
100 peptides produced by *Bacillus* sp. Taken together,  $\sigma^W$  is induced by envelope stress and protects the  
101 cell against antibiotics and bacteriocins, especially if they have membrane-disruptive properties, e.g.  
102 by altering membrane lipid composition [26].  $\sigma^X$  contributes to the resistance against cationic  
103 antimicrobial peptides (AMPs) by altering cell surface properties [27]. Accordingly, a *sigX* mutant is  
104 more sensitive to cationic AMPs such as nisin, which were not included in this study. The *dltA* operon  
105 (D-alanylation of teichoic acid) and *pssA* operon (biosynthesis of phospholipid) were previously shown  
106 to be most strongly activated by  $\sigma^X$  [27]. Both of the systems decrease the net negative charge of the  
107 cell envelope, reducing AMPs binding.  $\sigma^V$  is strongly and specifically induced by lysozyme and its  
108 induction provides lysozyme resistance [28]. Despite some regulatory overlap with  $\sigma^X$  at the level of  
109 promoter recognition,  $\sigma^V$  stress response presumably has evolved to defend against lytic enzymes.  
110 In contrast to the CESR functions described for the three ECFs above,  $\sigma^M$  plays a much more  
111 fundamental role in modulating the core PG biosynthesis and cell division machinery of *B. subtilis*,  
112 thereby maintaining the integrity of the CW in the presence of CES. While a *sigM* mutant is highly  
113 sensitive to  $\beta$ -lactams, its anti- $\sigma$  factor is encoded by an essential gene, indicating that the cell cannot  
114 tolerate a dysregulation of essential processes caused by the resulting upregulation of the  $\sigma^M$  regulon  
115 [25].  
116 Four out of 32 TCSs are directly involved in mediating the CESR of *B. subtilis*: LiaSR, BceRS, PsdRS, and  
117 ApeRS [29]. The TCS LiaRS of *B. subtilis* was originally named for lipid II cycle interfering antibiotic

118 response regulator and sensor. Accordingly, the LiaR target operon, *liaIH*, can be strongly induced in  
119 the presence of the antibiotics that interfere with the lipid II-cycle [30]. In addition, membrane-active  
120 compounds such as daptomycin also activate the Lia response [31, 32], most likely by indirectly  
121 interfering with lipid II. But despite extensive studies, the true nature of the signal provoking the Lia  
122 system and also its biological role remain poorly understood. BceRS, PsdRS and ApeRS are three  
123 paralogous TCSs that are specifically induced by and mediate resistance against CESR. They are  
124 functionally and genetically associated with ABC transporters, and together form a unique type of  
125 AMPs detoxification modules that are widely conserved in *Firmicutes* bacteria [33]. AMPs bind to and  
126 are sensed through the cognate ABC transporters, which indirectly activates the TCS. In response, the  
127 corresponding ABC transporter genes are strongly induced and their gene products remove the AMP  
128 from the cell surface, thereby mediating resistance [34, 35]. All of these systems show a high substrate-  
129 specificity [36].

130 Two additional TCSs have regularly been associated with the CESR of *B. subtilis*. The TCS CssRS (control  
131 secretion stress regulator and sensor) controls the cellular responses to protein secretion stress in *B.*  
132 *subtilis* [37]. The stress of high-level production of secretory proteins mounts the CssRS-dependent  
133 induction of *htrA* and *htrB*, which encode extracellular membrane-anchored quality control proteases  
134 [37, 38]. The TCS WalRK orchestrates CW homeostasis in *B. subtilis* and is essential for its viability [39].  
135 It was originally characterized in *B. subtilis*, but is widely conserved in, and specific to *Firmicutes*  
136 bacteria, including a number of important pathogens [39-43]. In *B. subtilis*, WalRK controls a set of  
137 genes that are either activated or repressed by the WalR response regulator [39, 44, 45]. When CW  
138 metabolism is particularly active, e.g. during the exponential growth phase when cells are rapidly  
139 growing and dividing, the WalRK system is highly activated. As a result, genes positively regulated by  
140 WalR, such as *cwIO* and *lytE* (encoding the co-essential D,L-endopeptidase type autolysins LytE and  
141 CwIO involved in PG elongation), *yocH* (peptidoglycan amidase) and *ftsAZ* (cell division), show a higher  
142 expression level to ensure high CW plasticity for cell growth [46-48]. In contrast, genes negatively  
143 regulated by WalR, such as *iseA* (inhibitor of LytE and CwIO) and *pdaC* (peptidoglycan deacetylase C),  
144 are repressed [39, 49, 50]. In non-diving cells (stationary phase), WalRK activity is tuned down.  
145 Repressed genes of the WalR regulon will be released from repression, while the activated genes are  
146 transcriptionally downregulated. As a consequence, CW turn-over is reduced, in line with the arrested  
147 CW growth and halted cell division.

148  
149 **Profiling the CESR of *B. subtilis*.** While numerous studies have been performed in the past to analyze  
150 the transcriptional response of *B. subtilis* to individual CW antibiotics (summarized in [51]), many are  
151 from the early days of transcriptomics and are often of low quality due to the experimental procedures,  
152 parameters and platforms applied. The sensitivity and dynamic range of early macro- and microarrays

153 were far from what can be resolved with current approaches. But even more importantly is the choice  
154 of conditions for stress response experiments. Sublethal antibiotic concentrations and short incubation  
155 times between induction and harvest are the two most critical parameters to ensure that only the  
156 specific, that is the primary, transcriptional CESR is monitored [51]. Signal transduction and gene  
157 regulation are inherently fast processes and full responses to antibiotic challenge can be monitored  
158 already after 3-5 min [52, 53]. In contrast, higher antibiotic concentrations (at or even above the MIC)  
159 and prolonged exposure to the antibiotic (30-60 mins were often applied) leads to an accumulation of  
160 cellular damage and increasingly unspecific transcriptomic signatures. In the worst case, the specific  
161 primary responses are masked or already shut off [51]. Variations in experimental procedures also  
162 hamper a meaningful comparison between different transcriptome profiles, thereby ultimately  
163 preventing to gather a comprehensive picture of the CESR response, when challenged with different  
164 CW antibiotics. Moreover, virtually all previous studies refer to the initial *B. subtilis* genome sequence  
165 [54], which contained numerous errors and missed many genomic features, such as small non-coding  
166 RNAs that were only uncovered much later in the course of updating the genome sequence [55].

167  
168 This study aims at revealing the genome-wide transcriptional response of *B. subtilis* to a set of PG  
169 synthesis inhibitors and providing a comprehensive picture of the CESR of *B. subtilis* from a  
170 transcriptomic point of view. A set of compounds that interfere with all three stages of PG biosynthesis,  
171 the initial intracellular steps (fosfomycin and D-cycloserine), the membrane-associated lipid II-cycle  
172 (tunicamycin, bacitracin, vancomycin) as well the final extracellular steps (moenomycin and penicillin  
173 G) (Fig. 1) were used at sublethal concentrations. Lysozyme was also included as an agent that destroys  
174 the already made murein sacculus. In order to analyze the performance of our profiling efforts and  
175 validate the data, we applied in parallel two independent current methods of transcriptional profiling:  
176 RNAseq and the latest generation of *B. subtilis* tiling arrays, which had previously been established as  
177 the gold standard for studying gene expression levels on a global scale [56]. Each stimulon was carefully  
178 dissected and comparatively analyzed to uncover the role of ECFs and TCSs in the CESR. ECF regulons  
179 were refined and a set of *B. subtilis* whole-cell biosensors were constructed and evaluated for their  
180 functionality.

181

## 182 Results

### 183 Experimental design, data processing and identification of CESR-induced genes

184 Initially, the inhibitory activity of the eight antimicrobial compounds was carefully analyzed on wild  
185 type *B. subtilis* cells growing in LB medium at 37°C, in order to determine the appropriate sub-lethal  
186 concentrations to be used for our transcriptomic experiments (Fig. S1). Cells at mid-exponential growth  
187 phase ( $OD_{600} \approx 0.4$ ) were then treated for 10 min, and samples were collected for RNA extraction, cDNA  
188 library preparation and either RNA sequencing or tiling array hybridization. The resulting raw  
189 sequencing reads and hybridization patterns, respectively, were analyzed to identify compound-  
190 specific and common changes of gene expression caused by the eight antibiotics, using untreated  
191 samples as negative control (see Experimental Procedure for details).

192 The mapping of expression signals was referred to the annotation file “BSGatlas\_v1.0.gff” from  
193 BSGatlas (<https://rth.dk/resources/bsgatlas/>), which contains 4773 generic features including coding-  
194 and non-coding genes, UTRs, transcripts, TSSs, and terminator structures [57]. SubtiWiki  
195 (<http://subtiwiki.uni-goettingen.de/>) was used as the “official” reference for both gene annotations  
196 and the definition of regulons, as this platform is manually curated to continuously incorporate and  
197 update the latest findings on *B. subtilis* [58].

198 We first applied a threshold of four-fold change of gene expression in at least one treatment condition  
199 as an initial filter. This resulted in 307 genes, 66 ncRNAs, 14 new RNA features and 22 novel transcripts  
200 that were differentially expressed in the RNAseq dataset as compared to a non-treated control (Table  
201 S1) and 212 genes and 84 ncRNAs differentially expressed in the tiling array dataset (Table S2). This  
202 corresponds to 8.6% and 4.4% of all expressed genes in our RNAseq and tiling arrays analysis,  
203 respectively. Next, the transcripts with very low basal expression (less than 10 transcriptional reads on  
204 average for RNAseq (Table S1) or a level of expression under 9 for tiling arrays) were manually removed  
205 to avoid irrelevant fold-change of gene expression. In addition, the 20 rRNAs were also removed  
206 because of their high and consistent expression levels (Fig. S2). The remaining 327 differentially  
207 expressed transcripts that include 298 genes, 16 ncRNAs, 7 new RNA features and 6 novel transcripts  
208 were then subjected to in-depth analyses. Hierarchical clustering analysis was performed using the  
209 Heatmap2 package in R program. This unsupervised clustering algorithm divided the large list of  
210 differentially expressed genes into 11 clusters of similar patterns (C1 to C11, Table S3). These clusters  
211 correlate with (combinations of) distinct regulons and allowed visualizing the specific expression  
212 patterns within each stimulon, thereby enabling the analysis of specific expression signatures based  
213 on the activation of distinct signaling pathways (Fig. 2, RNAseq and Fig. S3 tiling array). Graphical  
214 representations of the individual stimulons are provided in Fig. 3. For reasons of clarity and simplicity,  
215 only RNAseq data are shown hereafter in the main figures, while the corresponding tiling array data



216 are provided in supplemental material (tables S5,7,9,11,13,15,17,19). The good correlation of both  
217 approaches is illustrated in the regulon-specific expression data provided in Fig. 4-Fig. 6.

218  
219 **Inhibition of membrane-anchored steps of PG synthesis induces a strong CESR, in contrast to**  
220 **cytoplasmic and extracellular steps**

221 In both the RNAseq and tiling array data, CW antibiotics inhibiting the early cytoplasmic steps  
222 (fosfomycin and D-cycloserine) and the extracellular crosslinking reactions (moenomycin and penicillin  
223 G) did not trigger a pronounced transcriptional response. In contrast, antibiotics interfering with the  
224 membrane-anchored steps (bacitracin, tunicamycin and in particular vancomycin) provoked strong  
225 and specific responses (Fig. 2, Fig. 3 and **Erreur ! Source du renvoi introuvable.**3). This dominant  
226 feature may reflect the membrane-proximate perception of envelope stress by the TCSs and ECFs  
227 involved (see below). Lysozyme, which actively damages the CW, was also a strong CESR inducer, with  
228 a transcriptional signature that seemed to almost anti-correlate with the vancomycin stimulon. The  
229 top five genes triggered by each stimulus are present in Table 1. All genes showing a fold-change  
230 difference of at least two (fosfomycin, D-cycloserine, moenomycin and penicillin G) or five  
231 (tunicamycin, bacitracin, vancomycin and lysozyme) have been summarized in the compound-specific  
232 4 to Table S19. Each of the eight antibiotics caused between 0 and 275 genes or ncRNAs to be  
233 differentially expressed as compared to non-treated control cells. 12/1 genes were differentially  
234 expressed in response to fosfomycin, 11/0 to D-cycloserine, 103/18 to tunicamycin, 81/61 to  
235 bacitracin, 275/110 to vancomycin, 79/0 to moenomycin and 131/22 to lysozyme in the RNAseq/tiling  
236 array data.

237  
238 **The stimulons: antibiotic-specific transcriptional profiles of *B. subtilis***

239 **Fosfomycin**, which targets the first committed intracellular step of PG precursor biosynthesis, the  
240 conversion of UDP-GlcNAc to UDP-MurNAc by MurA (Fig. 1), provoked only a minor response in *B.*  
241 *subtilis* (Fig. 3A). Only the *pyr* operon (Fig. 2, cluster 7), involved in pyrimidine metabolism, was induced  
242 above 5-fold (Fig. 3A, and Table S4 and Table S5). A weak induction of *pdaC* and *iseA*, negatively  
243 controlled by WalR (Fig. 6), as well as genes associated with glucosamine utilization (*gamAP*) are in line  
244 with responding to an inhibition of PG precursor biosynthesis. PdaC is a PG deacetylase that confers  
245 lysozyme resistance [49], while IseA acts as an inhibitor of PG hydrolases that reduces the rate of  
246 antibiotic-induced cell death [50]. No ECF-dependent gene expression was observed in response to  
247 fosfomycin, nor did this compound trigger any of the four typical TCS involved in the CESR of *B. subtilis*.  
248 **D-cycloserine** inhibits the formation of the dipeptide D-alanyl-D-alanine (D-Ala-D-Ala) (Fig. 1). The  
249 response of *B. subtilis* to D-cycloserine was even weaker, but otherwise comparable to that to  
250 fosfomycin. The *pyr* and *gamAP* operons were weakly induced (Fig. 3B and Table S6). Like fosfomycin,

251 D-cycloserine is known as a  $\sigma^W$  inducer [52] but this activation was not detected in our experimental  
252 conditions, after 10 min of treatment.

253 **Tunicamycin** targets the first membrane-associated step of PG biosynthesis by preventing the  
254 formation of lipid I from UDP-MurNAc-pentapeptide [59]. Additionally, tunicamycin also interferes  
255 with the formation of wall teichoic acids [14]. Previously, tunicamycin was shown to weakly induce  $\sigma^{ECF}$   
256 and the Lia system [30, 52, 60, 61], which could be confirmed by our transcriptomic study. ECF-  
257 dependent gene expression was primarily orchestrated by  $\sigma^W$  (Fig. 3C), but – to a weaker extent – also  
258 by  $\sigma^M$  (Fig. 4). A moderate activation of the Lia system by tunicamycin was also detected (Fig. 5), which  
259 is consistent with an earlier study [30]. Surprisingly, many AhrC- and CodY-controlled operons related  
260 to amino acids metabolism (e.g. biosynthesis of arginine, leucine, branched-chain amino acids,  
261 methionine, and cysteine) were amongst the most highly induced genes (Fig. 2 cluster 3, Fig. 3C and  
262 Table S8 and Table S9). Finally, the WalR-dependent genes *pdaC* and *iseA*, also induced by fosfomycin  
263 and D-cycloserine, and the CssR-dependent secretion stress-inducible genes *htrA* and *htrB* were also  
264 activated (Fig. 3C, Fig. 5, Fig. 6, Table S8 and Table S9). Tunicamycin therefore strongly triggered amino  
265 acid metabolism genes and, to a lesser degree, the induction of  $\sigma^W$  and  $\sigma^M$  regulons, as well as affecting  
266 the TCSs LiaRS, WalRK, and CssRS.

267 **Bacitracin** prevents the recycling of the lipid carrier undecaprenol (Fig. 1). In line with previous studies  
268 [53], bacitracin strongly activated the two operons *lialH-liaGFSR* and *bceAB*, which are under control  
269 of the TCS LiaRS and BceRS, respectively (Fig. 2 cluster 6, Fig. 3D, Table S10 and Table S11). The *bceAB*  
270 operon encodes the ABC transporter BceAB, which acts as the primary bacitracin resistance  
271 determinant, while LialH provide a secondary layer of resistance [24, 53, 62] (Fig. 5). As observed  
272 previously, two BceRS-paralogs, PsdRS and ApeRS, were also weakly induced, presumably through  
273 cross-activation by BceRS [52, 62]. The ECF-dependent response to bacitracin was less pronounced  
274 than the TCS-mediated response and primarily mediated by  $\sigma^M$  and to a lesser extent by  $\sigma^W$  and  $\sigma^V$  (Fig.  
275 4), in line with previous observations [53]. Together, these ECFs control induction of *bcrC*, encoding a  
276 second undecaprenyl pyrophosphate phosphatase that functions as a bacitracin resistance  
277 determinant [60, 63].

278 Since bacitracin is complexed with Zn(II) ions, which are also required for this antibiotic to be  
279 biologically active [64], bacitracin treatment also activated the CrzA-mediated toxic metal ion stress  
280 response by inducing *cadA* and the *czcD-czcO* operon (Table S10 and Table S11), which mediate  
281 resistance against them [65]. All of the above responses have been observed and characterized  
282 previously [53]. In contrast, induction of *yrhH-fatR-yrhJ* (fatty acid biosynthesis) and *hisZGDBHAFI*  
283 (histidine biosynthesis) was observed for the first time in this study (Fig. 8, Table S10 and Table S11).

284 **Vancomycin** inhibits PG biosynthesis by binding to the D-alanyl-D-alanine dipeptide terminus of  
285 externalized Lipid II, thereby blocking glycan polymerization and cross-linking [18]. Vancomycin was

286 already known as a strong inducer of the CESR in *B. subtilis*, in particular the  $\sigma^W$  regulon [52]. Our  
287 results (Fig. 2 cluster 10, Fig. 3E and Fig. 7) are consistent with these findings. The LiaRS-regulated *lialH-*  
288 *liaGFSR* operon and the  $\sigma^W$  regulon predominated the primary response of *B. subtilis* to vancomycin  
289 (Fig. 3E, Table S12 and Table S13).  $\sigma^M$  and  $\sigma^V$  were also activated, but to a lesser degree (Fig. 4).  
290 Several signature genes of the vancomycin stimulon are related to inhibition of both PG synthesis and  
291 hydrolysis. The WalR-controlled PG hydrolases were inhibited by induction of the *iseA* gene  
292 (modulating autolysins activity) and repression of the co-essential *lytE* and *cwIO* (encoding DL-  
293 endopeptidases), and of *ydjM* (encoding a CW-associated protein). In parallel, genes involved in PG  
294 synthesis (e.g. *murE-mraY-murD-spoVE operon*, *mbl*, *dacA*) were also repressed. Interestingly, *yrhH-*  
295 *fatR-yrhJ* was strongly induced, as observed for bacitracin. The CsrRS-dependent protein quality  
296 control genes *htrAB* were also induced by vancomycin, as by many other CW antibiotics (Fig. 5).  
297 In contrast to the other antibiotics analyzed in this study, different vancomycin concentrations were  
298 used between RNAseq (1  $\mu\text{g/ml}$ ) and tiling array (0.25  $\mu\text{g/ml}$ ) studies. While this 4-fold difference in  
299 antibiotic concentration did not change the overall picture of the primary CESR (the same regulons  
300 were identified in both vancomycin stimulons), quite a number of its genes showed differences in the  
301 overall induction strength, which was mostly higher at 1  $\mu\text{g/ml}$  (Fig. 4 and Fig. 8). More importantly, it  
302 resulted in significant differences in the secondary, less specific, global responses (Fig. 7, Table S12 and  
303 Table S13): The  $\sigma^B$ -dependent general stress response was weakly activated at 1  $\mu\text{g/ml}$  vancomycin in  
304 the RNAseq experiments, indicating that the primary and more specific responses did no longer  
305 provide enough protection at this higher antibiotic concentration [66]. Moreover, the stringent  
306 response was more severely affected at higher vancomycin concentrations, as indicated by the  
307 repression of many ribosomal protein-encoding genes in the RNAseq data (Fig. 3E and Table S12).  
308 Taken together, vancomycin triggers a very strong CESR in *B. subtilis*, which is largely mediated by the  
309 TCS LiaRS and WalKR,  $\sigma^W$  and (at higher vancomycin concentrations as observed in RNAseq) the  $\sigma^B$ -  
310 dependent general stress response. The results obtained so far demonstrate that global expression  
311 studies on antibiotic stress are rather robust to different technological platforms, but strongly affected  
312 by the antibiotic concentrations applied. Secondary, global responses are usually induced at higher  
313 concentrations by the accumulating damage caused by antibiotic action [51].  
314 **Moenomycin** targets the glycosyltransferase activity of aPBPs [20]. Similar to the inhibition of the  
315 intracellular steps of PG biosynthesis, only a weak transcriptional response is observed for this  
316 antibiotic. The *pyr* operon (involved in uracil metabolism) was the only locus to be repressed  $\geq 5$ -fold,  
317 while no gene was induced  $\geq 5$ -fold, in line with a previous study [67] (Fig. 3F, Table S14 and Table S15).  
318 A weak activation of  $\sigma^M$  and  $\sigma^V$  was nevertheless detectable (Fig. 3 and Fig. 4). Interestingly, the  
319 strongest induction was observed for the *yrhH-fatR-yrhJ* locus, which is jointly regulated by  $\sigma^M$ ,  $\sigma^W$ ,  $\sigma^X$   
320 and FatR. Other strongly induced genes were also co-regulated by several ECFs (Table S14 and Table

321 S15). Of the different ECF  $\sigma$  factors,  $\sigma^M$  was reported to be the only one contributing to moenomycin  
322 resistance in *B. subtilis*: A *sigM* deletion strain was much more sensitive to moenomycin than any other  
323  $\sigma^{ECF}$  mutation and only the overexpression of  $\sigma^M$  in the  $\Delta 7ECF$  mutant was able to restore the resistance  
324 of *B. subtilis* to this compound [68]. But overall, inhibiting the TG activity of aPBPs by moenomycin only  
325 triggered a minor response in *B. subtilis*.

326 **Penicillin G** and related  $\beta$ -lactams inhibit the TP activity of so-called penicillin-binding-proteins (PBPs).  
327 Again, the response of *B. subtilis* to this extracellular inhibitor of PG biosynthesis was not very  
328 pronounced (Fig. 2, Fig. 3G, Table S16 and Table S17). The  $\sigma^W$  regulon was activated, with the *yuaF*-  
329 *floT-yuaI* operon being the only one induced  $\geq 5$ -fold.  $\sigma^M$  was also slightly induced by penicillin G,  
330 while  $\sigma^X$  and  $\sigma^V$  were not responsive (Fig. 3G and Fig. 4). The *apeAB-yxeA* operon, which is controlled  
331 by the TCS ApeRS, was surprisingly induced 2.5 fold (Fig. 3G and Fig. 4) since ApeRS usually responds  
332 to antimicrobial peptides of eukaryotic origin. Nevertheless, our data indicate that penicillin G is a weak  
333 inducer of the CESR of *B. subtilis*, in line with previous reports [69].

334 **Lysozyme stimulon**. Lysozyme kills bacteria by cleaving the  $\beta$ -1,4-glycosidic bonds between the  
335 MurNAc and GlcNAc, resulting in cell lysis [70]. It is a strong inducer of  $\sigma^V$  through direct binding of  
336 lysozyme to the membrane-anchored anti- $\sigma$  factor RsiV [28, 71]. The activation of  $\sigma^V$  confers lysozyme  
337 resistance through OatA-dependent PG O-acetylation (encoded in *sigV-rsiV-oatA-yrhK* operon) and  
338 DltABCDE-dependent D-alanylation of teichoic acids [71, 72], which is controlled by  $\sigma^X$ ,  $\sigma^V$  and  $\sigma^M$ .  
339 Indeed, we observed a >40-fold induction of the *sigV* operon upon lysozyme addition (Fig. 3H and Table  
340 1), while the *dlt* operon was only induced approximately two-fold (Table S18 and Table S19). Additional  
341 ECFs were also induced by lysozyme, including  $\sigma^M$ ,  $\sigma^X$  and  $\sigma^W$  (Fig. 3H and Fig. 4). A strong induction  
342 was again observed for *iseA* and *pdaC* (approx. 30- and 13-fold, respectively). Interestingly, the CzrA-  
343 controlled *czcD-czcO* operon and *cadA* gene, which normally respond to metal ion stress [65], were  
344 strongly activated by lysozyme, as already observed for bacitracin. While the induction by bacitracin  
345 was due to the Zn(II) ions coordinated by this antibiotic, the reason for the CzrA response to lysozyme  
346 will require further investigations. Other genes induced strongly and exclusively by lysozyme include  
347 the *maeA-ywkB* operon and *maeN* gene, which are controlled by TCS MalRK involved in malate  
348 utilization [73], and the CssR-controlled genes *htrA* and *htrB*, which were also induced by tunicamycin.  
349 Despite the severe CW damage caused by lysozyme, the  $\sigma^B$ -dependent general stress genes was  
350 strongly repressed by lysozyme, while stringent response-associated genes were upregulated. Taken  
351 together, our data show that disruption of CW by lysozyme triggered a strong and complex response  
352 with the significant activation of  $\sigma^V$  and  $\sigma^M$ , as well as the involvement of TCS WalRK.

353

## 354 Refinement of the ECF $\sigma$ factor regulons

355 The  $\sigma^{\text{ECF}}$ -dependent antimicrobial resistance network constitutes one of the two major regulatory  
356 routes mediating the CESR in *B. subtilis*. Of the seven  $\sigma^{\text{ECF}}$  factors encoded in the genome of *B. subtilis*,  
357 four ( $\sigma^{\text{W}}$ ,  $\sigma^{\text{M}}$ ,  $\sigma^{\text{X}}$  and  $\sigma^{\text{V}}$ ) are well-understood in terms of their roles in cell envelope homeostasis and  
358 antibiotic resistance. Their regulons have been extensively investigated and are well determined [25,  
359 74, 75]. Remarkably, a significant extent of regulatory overlap was observed due to the similarities of  
360 promoter sequences recognized by those  $\sigma^{\text{ECF}}$  factors [60, 76-78]. The resulting functional redundancy  
361 [79] still poses a challenge in determining the contribution of individual  $\sigma^{\text{ECF}}$  factors to the expression  
362 of genes assigned to multiple regulators. We therefore attempted to refine the  $\sigma^{\text{W}}$ ,  $\sigma^{\text{M}}$ ,  $\sigma^{\text{X}}$  and  $\sigma^{\text{V}}$   
363 regulons by integrating the comprehensive transcriptional profiles generated in this study with the  
364 previously established detailed information on each regulon and their regulatory overlap. Towards this  
365 goal, we (i) determined the major regulator of genes under control of multiple  $\sigma^{\text{ECF}}$  factors based on  
366 the distinct expression pattern of each regulon (Fig. 4), (ii) reevaluated the members of the four  $\sigma^{\text{ECF}}$   
367 regulons according to their response to the different stresses (Table 2), and (iii) searched for novel  
368 candidates for the four  $\sigma^{\text{ECF}}$  regulons via hierarchical clustering analysis (Fig. S45 and Table S2020).  
369 Based on this combined analysis, five different groups of ECF-dependent genes could be identified  
370 (Table 2).

371 Group I includes genes that appear to have  $\sigma^{\text{M}}$  as their major regulator. They were induced by  
372 lysozyme, bacitracin and moenomycin. Some genes, such as *bcrC* and *divIC*, are regulated by additional  
373 ECFs.

374 Group II genes are primarily controlled by  $\sigma^{\text{X}}$ . This group of genes was only activated by lysozyme and  
375 repressed by vancomycin and sometimes also other CW antibiotics, such as bacitracin or moenomycin  
376 (Table 2). The overall response of  $\sigma^{\text{X}}$ -dependent genes appeared to be very weak to the stresses  
377 applied in this study.

378 Group III genes are exclusively regulated by  $\sigma^{\text{V}}$ . Most of the  $\sigma^{\text{V}}$ -dependent genes are also controlled by  
379  $\sigma^{\text{X}}$ ,  $\sigma^{\text{M}}$ , and  $\sigma^{\text{W}}$  [77], with only the *sigV* operon being exclusively regulated by  $\sigma^{\text{V}}$ . In this study, the *sigV*  
380 operon was most strongly induced by lysozyme, but also weakly by bacitracin, vancomycin and  
381 moenomycin (Table 2).

382 Group IV genes are controlled by  $\sigma^{\text{M}}$ , but may also be significantly regulated by other ECFs. Genes from  
383 within this group showed a broader inducer spectrum. While they are also partially controlled by  $\sigma^{\text{M}}$   
384 but are more strongly induced by vancomycin than the preferentially  $\sigma^{\text{M}}$ -dependent genes of Group I.  
385 Notably, they all have additional regulator(s) other than ECFs, such as  $\sigma^{\text{B}}$ , FatR, Spx, and WalR (Table  
386 2).  $\sigma^{\text{W}}$  seems to play only a secondary role in regulating genes of group IV. Genes in this group perfectly  
387 match the previously compiled list of genes that were  $\sigma^{\text{W}}$ -dependent but not significantly down-  
388 regulated in a  $\sigma^{\text{W}}$  mutant [80].

389 Finally, Group V includes all genes primarily (mostly exclusively) regulated by  $\sigma^W$  (Table 2), with the  
390 exception of *yceCDEFGH* operon, which is also regulated by  $\sigma^M$ ,  $\sigma^X$  and  $\sigma^B$  [74, 75, 81, 82]. The sequence  
391 alignment revealed that the promoters of these genes share characteristic sequence motifs at the -35  
392 and -10 regions (Fig. S5). In particular, the -10 region with “CGTA” motif is clearly distinct from the  
393 corresponding regions of other ECF-target promoters in *B. subtilis*, which more frequently show a  
394 “CGTC” motif.

395 Taken together, our analysis provides a comprehensive picture of ECF-dependent gene expression.  
396 While it confirmed most of the known ECF-target genes, it also identified potentially novel members  
397 of the  $\sigma^W$  regulon. The comprehensive analysis of the distinct expression patterns of the ECF regulons  
398 under different CESs enabled us to distinguish the partially overlapping ECF regulons and allowed  
399 determining the major regulators for the genes co-regulated by different ECFs.

400

#### 401 **The role of TCSs in mediating CESR of *B. subtilis***

402 Four TCSs represent the second major regulatory principle coordinating CESR of *B. subtilis*, LiaRS,  
403 BceRS, PsdRS and ApeRS [29]. In addition to these directly CESR-inducible TCSs, the homeostatic TCS  
404 WalRK, which coordinates the CW metabolism, and CssRS, which mediates protein secretion stress,  
405 are also induced by some triggers of CES.

406 **Induction of LiaRS by inhibitors of lipid II-cycle.** In the present study, the strong induction of the Lia  
407 system by bacitracin and vancomycin was confirmed (Fig. 5) [83]. Tunicamycin also activated this  
408 system, but to a lesser extent, which is also consistent with a previous study [30]. While all three  
409 compounds induced *liaIH-liaGFSR*, LiaR was also reported to control two additional targets, the *yhcYZ-*  
410 *yhdA* operon and *ydhE* gene, as suggested by the LiaR-binding sites present upstream of their  
411 promoters [53, 84, 85]. The *yhcY* operon was induced weakly by bacitracin (~2-fold) in this study,  
412 whereas *ydhE* did not appear to be responsive to any condition, in line with previous studies [53, 84,  
413 85].

414 **The response of the detoxification modules controlled by BceRS, PsdRS and ApeRS.** In the present  
415 study, the *bceAB* operon was specifically and strongly induced by bacitracin (Fig. 5). It was suggested  
416 that the BceAB transporter protects the cell by target-protection via transiently freeing lipid II-cycle  
417 intermediates from bacitracin [86]. Other lipid II-targeting AMPs, such as the lantibiotics nisin and  
418 subtilin, induce the paralogous *psdAB* operon, which is controlled by PsdRS, and responds in a similar  
419 way to these two compounds [36]. The *psdAB* operon showed a moderate activation by bacitracin in  
420 the present study, which is consistent with previous studies [53, 87] and most likely due to a regulatory  
421 cross-activation of *psdAB* expression via BceRS. ApeRS is the least well studied among these three TCSs.  
422 So far, the human-derived cationic antimicrobial peptide LL-37 [88], and *Hermetia illucens* larval  
423 extract [89] are the only known stimuli of ApeRS. In this study, a ~2.5 fold induction of its target operon,

424 *apeAB-yxeA*, was observed during penicillin G treatment (Fig. 5). The physiological relevance of this  
425 result needs to be further investigated. No other compound was able to activate this TCS.

426 **The CESR of the secretion stress system CssRS.** The CssRS system is part of the quality control  
427 mechanisms in protein secretion [37]. The present study demonstrates that the *htrAB* operon was  
428 induced by bacitracin, lysozyme, tunicamycin and vancomycin. These results suggest that interfering  
429 with membrane-anchored steps of CW biosynthesis also negatively affects protein secretion, thereby  
430 generating a stress that is sensed by CssS. Activation of CssRS as part of the CESR of *B. subtilis* has  
431 previously also been reported for rhamnolipid treatment [51]. This result demonstrates the close  
432 relationship between shuttling CW building blocks and proteins to the outside of the cell, indicative  
433 for a limited capacity of the membrane for accommodating such export processes, which is an  
434 underappreciated of CES that will require further investigations.

435 **WalRK-dependent CW homeostasis is negatively affected by CES.** In the presence of all antibiotics of  
436 this study, the genes *cwI*, *lytE*, *yocH* and *ydjM*, which are positively regulated by WalR [39, 44],  
437 exhibited overall downregulated expression (Fig. 6), reflecting the reduction in CW metabolism and  
438 suggesting deregulated PG hydrolytic activity when PG synthesis is inhibited. Additionally, *ftsEX*, which  
439 is required for CwI activity [90], was downregulated around five-fold by vancomycin (Table S12).

440 Conversely, *iseA*, *pdaC* and *sasA*, which are negatively regulated by WalR [39], were released from  
441 WalR repression and hence increased in expression (Fig. 6). The strong (30-fold) induction of *iseA* by  
442 lysozyme was observed for the first time. Likewise, *pdaC*, which confers lysozyme resistance via de-N-  
443 acetylation of PG [91], was also strongly induced by lysozyme. Noteworthy, the response of *pdaC* shows  
444 some compound-specificity, in contrast to the almost overall upregulation of *iseA* expression in the  
445 presence of all CW inhibitors (Fig. 6). Taken together, the response of WalR-target genes shows that  
446 WalRK activity was tuned down to reduce CW metabolism in response to the CES-dependent  
447 interference with CW synthesis.

448

#### 449 **Signature inductions of the CESR in *B. subtilis***

450 In addition to a comprehensive insight into the regulatory processes, our genome-wide transcriptional  
451 profiles on the CESR of *B. subtilis* to different CW antibiotics also unveiled marker genes that were  
452 particularly responsive under CES (Fig. 8). Such genes, or rather their target promoters, represent  
453 useful candidates for the development of whole-cell biosensors, which are stimulus-specific reporter  
454 strains that can be applied for searching for novel antimicrobial compounds [92].

455 The LiaRS-dependent *liaIH* operon has drawn extensive attention because of strong response of up to  
456 1000-fold induction to antimicrobial agents that mostly interfere with lipid II-cycle of PG biosynthesis  
457 [30, 53] (Fig. 8). Due to its low basal expression level, the *liaIH* promoter ( $P_{liaI}$ )-based biosensor is well-  
458 established for the identification of cell envelope-active compounds [84, 93].

459 The genes *yuaF-floT-yuaI*, *yeaA-ydjP(-ydjO)*, *pbpE-racX*, *pspA-ydjGHI*, *yvlABCD* and *fosB* are under  
460 control of  $\sigma^W$ , which was strongly activated by vancomycin (Fig. 8). The ***yuaF* operon**, was the most  
461 sensitive member of the  $\sigma^W$  regulon. It is involved in the control of membrane fluidity, which affects  
462 CW biosynthesis [94]. The ***yeaA* operon** remains uncharacterized. The first gene of ***pbpE-racX* operon**  
463 encodes a penicillin-binding protein PBP4\* (endopeptidase), while *racX* codes for an amino acid  
464 racemase involved in the production of non-canonical D-amino acids [95]. The first gene of the ***pspA-***  
465 ***ydjGHI* operon** encodes the second phage shock protein A (PspA) homolog of *B. subtilis*, in addition to  
466 LiaH [84]. YvIC, encoded in the ***yvlABCD* operon**, was identified as a PspC homolog [96]. Finally, ***fosB***  
467 mediates fosfomycin resistance in *B. subtilis* [97].

468 The expression of the ***yrhH-fatR-yrhJ* operon** (which is partially involved in fatty acid metabolism [98])  
469 is particularly interesting with regard to its broad spectrum of inducers in this study, including  
470 vancomycin; tunicamycin and moenomycin (Fig. 8). This operon is under control of multiple regulators  
471 ( $\sigma^M$ ,  $\sigma^W$ ,  $\sigma^X$  and FatR) and was assigned into the Group IV during the refinement of ECF  $\sigma$  regulons (Table  
472 2).

473 In addition to  $\sigma^{ECF}$ -dependent genes, the specific induction of the ***ytrABCDEF* operon** by vancomycin  
474 was noteworthy. This operon is induced by a narrow range of PG synthesis inhibitors blocking the lipid  
475 II precursor, including the glycopeptides vancomycin and ristocetin, which target the terminal D-Ala-  
476 D-Ala of the pentapeptide, the glycolipodepsipeptide ramoplanin, which sequesters lipid II, and  
477 plectasin, a fungal defensin that also targets lipid II [67, 99, 100]. Bacitracin was able to activate the *ytr*  
478 operon, but to a lesser extent (Fig. 8), consistent with earlier reports [53, 67].

479 The genes ***htrA*** and ***htrB*** encode membrane-anchored protein quality control proteases under control  
480 of the TCS CsrRS. The *htrA* gene was induced by tunicamycin, bacitracin, vancomycin and lysozyme  
481 (Fig. 8).

482 The WalR-dependent gene ***iseA*** was induced by a broad spectrum of antibiotics (Fig. 8). Previously,  
483 another member of the WalR regulon, ***sasA***, has been exploited as a biosensor for the discovery of  
484 novel CW-active compounds [101, 102]. The present study shows that *iseA* expression was even more  
485 sensitive than *sasA* towards cell envelope stress. Therefore, *iseA* may represent a promising candidate  
486 for the establishment of reporter strain derived from the WalR regulon.

487

#### 488 **Novel genomic features induced by CES**

489 In the course of the resequencing and especially the comprehensive systems biology analysis of *B.*  
490 *subtilis* gene expression [103], numerous novel genomic features were discovered, including non-  
491 coding 5'- leader transcripts (5'UTRs), or 3'-extension of genes and operons. Induction of these  
492 features is covered by this analysis for the very first time, the results are summarized in Table S21.  
493 Most novel features were differentially expressed in only one stress condition, and here the



494 discrepancies between RNAseq and tiling array data is much larger than for the rest of the transcripts.  
495 The most consistent of the strongly induced novel features are linked to known regulators of the CESR.  
496 This includes ECF-target genes and operons, e.g. S156 (5'UTR of *ddl*, S228 (5'UTR of *yebC*,  $\sigma^M$  /  $\sigma^V$   
497 regulon), S742 (5'UTR of *yoZ*,  $\sigma^W$  regulon), S843 (5'UTR of *recU*,  $\sigma^M$  regulon) or S659 (downstream of  
498 *fosB*). Other novel features with known regulators include S1268 (5'UTR of *htrB*, CsrR regulon) and  
499 S1275 (3'UTR of the *liaIHGFSR* operon, controlled by LiaR). But the relevance of induction of most of  
500 these over 100 novel features by cell wall antibiotics (as listed in Tab. S21) will require further  
501 investigations.

502

### 503 ***B. subtilis* biosensors for compound discovery**

504 Based on the signature gene expressions described above, a panel of eleven bioluminescence-based  
505 *B. subtilis* biosensors was constructed by transcriptionally fusing the promoters of signature genes to  
506 the *luxABCDE* cassette as a reporter gene (Table S22). We next tested the biosensors for their  
507 functionality, sensitivity, response dynamics using vancomycin as a model inducer. A strain with a  
508 promoterless *lux* cassette served as a negative control for background luminescence. All biosensors  
509 were induced with a dilution series of vancomycin ranging from 0 to 3  $\mu\text{g mL}^{-1}$  (see methods for details).  
510 Luminescence and cell density were monitored over time (Fig. S6) and the fold-induction for each  
511 condition was calculated (Fig. 9).

512 All biosensors exhibited a dose-dependent response to vancomycin and a good correlation – or even  
513 a higher dynamic range – was observed for the biosensors relative to the transcriptome data. e.g. the  
514  $P_{htrA}$  biosensor was activated approx. 40-fold, while only a five-fold induction of *htrA* expression was  
515 observed by RNAseq. Likewise, the  $P_{pbpE}$  biosensor was induced 33-fold, while only a nine-fold  
516 induction of *pbpE* expression was detected. In both cases, this was due to the induction kinetics, since  
517  $P_{htrA}$  and  $P_{pbpE}$  responded more slowly to vancomycin than other promoters (Fig. S6). Consequently, the  
518 highest induction value chosen for the biosensor assays occurred at 30-45 minutes post-induction,  
519 while the induction levels of *htrA* and *pbpE* in RNAseq were determined after 10 min of induction.

520 No major differences were observed between the sensitivity of the promoters to vancomycin. The  
521 threshold concentration for  $P_{yuaF}$  and  $P_{ytrA}$  induction was 0.05  $\mu\text{g mL}^{-1}$ , while all other promoters  
522 starting responding at 0.1  $\mu\text{g mL}^{-1}$  (Fig. 9 and Fig. S6). The maximum activity of most promoters  
523 occurred at 1  $\mu\text{g mL}^{-1}$  of vancomycin, while higher concentrations did neither increase nor decrease  
524 the promoter activity further. Only  $P_{liaI}$  activity was still increasing at 2 or even 3  $\mu\text{g mL}^{-1}$  of vancomycin.  
525 Conversely,  $P_{yvlA}$  exhibited the highest activity at 0.6  $\mu\text{g mL}^{-1}$ , followed by declined activity at higher  
526 concentration treatments.

527 Noteworthy,  $P_{iseA}$  – but not any other promoters – displayed increased activity at late-exponential  
528 phase, even in the absence of stimulus (Fig. S6), due to a negative regulation by WalRK. During

529 exponential phase, WalRK is highly active, thereby repressing *iseA* expression. With a decrease of CW  
530 growth at the onset of the stationary phase, WalRK activity is also declining, thereby releasing *iseA*  
531 from WalR repression. The  $P_{iseA}$  biosensor was also tested with penicillin G, and similar dose-response  
532 behavior was observed (Fig. S7).

533 This novel panel of *B. subtilis* biosensors expands the range of biosensors already available for CW  
534 antibiotics. Their functionality and performance were verified based on their dose-response behavior  
535 to vancomycin, but some additionally responded to other antibiotics such as bacitracin and  
536 moenomycin (Fig. S8), underscoring their potential to detect new cell envelope-active compounds to  
537 facilitate the discovery of novel antimicrobial compounds.

538

## 539 Discussion

540 Bacteria living in complex environments, like the soil, compete with numerous other species for  
541 ecological niches and the scarce nutrients. Biological warfare – in the form of antibiotics – is one aspect  
542 of this competition, which allows bacteria to strive and prosper in the face of competitors. PG synthesis  
543 is a prime target for many antibiotics, due to its crucial role, and cells need to continuously monitor its  
544 integrity, in order to mount swift responses in the case of envelope damage. For over two decades,  
545 the underlying regulatory network of the CESR has been thoroughly studied in the Gram-positive soil  
546 bacterium *B. subtilis* [24, 104], but a systematic and comparative analysis has been missing so far. Here,  
547 we presented the results of such a comprehensive and highly standardized transcriptomic profiling  
548 study. We chose eight antimicrobials, including seven CW antibiotics that inhibit PG synthesis from  
549 early cytoplasmic steps (fosfomycin, D-cycloserine) via the membrane anchored lipid II cycle  
550 (tunicamycin, bacitracin, vancomycin) to the extracellular polymerization steps (penicillin G,  
551 moenomycin) and lysozyme, which degrades the existing CW (Fig. 1). Highly standardized experimental  
552 conditions (inhibitory but sublethal antibiotic concentrations and only 10 min induction) were chosen  
553 to exclusively monitor the primary, that is, initial antibiotic-specific responses. Moreover, two  
554 independent state-of-the-art transcriptomic technologies, RNAseq and the latest generation of tiling  
555 array, were applied in parallel to solidify the data and exclude technical biases. This approach enabled  
556 us gaining a comprehensive picture of the CESR of *B. subtilis*, providing an unsurpassed resolution on  
557 how an organism perceive threats and damages to its envelope. By mapping the transcripts on the  
558 updated genome sequence, we were also able to identify novel features, such as non-coding RNAs,  
559 even for stimulons that had been thoroughly analyzed in the past, such as the vancomycin or bacitracin  
560 stress responses. Taken together, our work provides a comprehensive reference analysis for future  
561 studies on the CESR in *Bacillus* species and related Firmicutes bacteria.

562 Applying two independent technologies for monitoring transcriptome profiles enabled us to both  
563 validate the data and also identify potential technical biases in our analysis. While RNAseq is currently

564 the most widely used standard for monitoring genome wide transcriptional profiles, high-resolution *B.*  
565 *subtilis* tiling arrays were thoroughly evaluated in the largest systems biology study for this organism  
566 [103], and served as an internal standard for our work. Overall, both approaches resulted in highly  
567 comparable datasets (Figs. 4, 5, 6, 8), demonstrating the robustness of transcriptomic studies,  
568 irrespective of the specific technology applied to quantify the transcripts. In contrast, the experimental  
569 conditions applied for cultivating the cells are highly critical, as shown by the differences found in the  
570 vancomycin stimulons when the antibiotic concentration varied by only a factor of four (0.25 vs. 1  
571  $\mu\text{g/ml}$  vancomycin). While the overall pattern was comparable, the higher antibiotic concentration  
572 resulted in higher fold-induction of the target genes and also in the additional induction of secondary,  
573 less specific responses, such as the SigB-dependent general stress response (Fig. 7).

574 Remarkably, applying standardized and comparable conditions to seven antibiotics that interfere with  
575 successive steps of PG synthesis also highlighted how the resulting stresses are perceived by the  
576 regulatory systems involved in orchestrating the CESR in *B. subtilis*. While a strong and differentiated  
577 response was observed for all compounds interfering with membrane-associated steps of PG synthesis  
578 (tunicamycin, bacitracin, vancomycin), for the compounds inhibiting either cytoplasmic (fosfomycin,  
579 D-cycloserine) or extracellular steps (moenomycin, penicillin G) no clear primary transcriptional  
580 signatures were observed and none of the known CESR systems was significantly triggered (Figs. 2-6).  
581 The strong and differential response to antibiotics interfering with membrane-anchored steps of PG  
582 synthesis is well documented [51-53]. It highlights the key role of the lipid II cycle as the bottleneck  
583 process in PG synthesis. By blocking this process, PG synthesis becomes dramatically dysbalanced:  
584 while soluble PG precursors accumulate on the cytoplasmic side, the growing murein sacculus is  
585 depleted for building blocks, and the action of PG hydrolases, which precedes but is normally well-  
586 coordinated with the incorporation of new material, gets deregulated and weakens the CW further. In  
587 addition to the almost instant effect that blocking the lipid II cycle has on PG biosynthesis, the site of  
588 this inhibition at the membrane is also ideally suited for perception by the membrane-anchored  
589 sensors of CES, e.g. the sensor kinases and the anti- $\sigma$  factors (or the proteases degrading them). Our  
590 transcriptional profiles strongly suggest that the CESR of *B. subtilis* has specifically evolved to  
591 immediately perceive interference with the lipid II cycle as the most reliable indicator of future CW  
592 damage. This hypothesis is in agreement with numerous additional transcriptomic studies from both  
593 Gram-positive and Gram-negative bacteria that draw a similar picture [51].

594 In contrast, interfering with cytoplasmic or extracytoplasmic steps is hardly detected by the cells at  
595 first, at least under the chosen experimental conditions. In the case of fosfomycin and D-cycloserine,  
596 the pool of soluble CW precursors was most likely not yet depleted after 10 min to significantly affect  
597 the successive steps, such as the lipid II cycle, and elicit a stronger transcriptional response. While using  
598 longer times between antibiotic induction and cell harvest might have resulted in a stronger and

599 clearer transcriptional profile, it was not the aim of this study to monitor downstream transcriptional  
600 effects of metabolic depletion, but rather to provide a comprehensive picture of the primary CESR of  
601 *B. subtilis*. Towards this end, our data clearly indicates that the initial, cytoplasmic reactions do not  
602 represent suitable stimuli to provide the cell with a sensitive read-out for CES. The poor primary (within  
603 10 min) response to the extracellular inhibitors of CW biosynthesis moenomycin and penicillin, which  
604 was also observed for other bacteria [51], might result from the plasticity of the PG meshwork to adapt  
605 to changing, often challenging, environmental conditions, favored by the multiplicity and often  
606 redundancy of the main players. TP and TG reactions are tightly coordinated between them and with  
607 the action of PG hydrolases, in order to incorporate new building blocks in the dynamically growing PG  
608 network [105]. In rod-shaped bacteria this process is coordinated by combining the necessary enzymes  
609 in highly motile PG biosynthetic complexes that are organized by cytoskeletal elements. Sidewall  
610 elongation is effected by the Rod complex, associated to the actin homolog MreB, and septum  
611 formation is effected by the divisome, associated to the tubulin homolog FtsZ [105, 106]. In *B. subtilis*,  
612 PG synthesis is additionally mediated by aPBPs (bifunctional PBPs with both TG and TP activity)  
613 functioning outside these complexes [107]. Moenomycin targets the glycosyltransferase activity of  
614 aPBPs [20] but not of the essential SEDS glycosyltransferases RodA and FtsW that are associated to the  
615 Rod complex and to the divisome, respectively. In agreement with this, in *B. subtilis* aPBPs are not  
616 essential and PG synthesis continues in moenomycin-treated cells [108]. Thus, the absence of a rapid  
617 transcriptional response when sublethal concentrations of moenomycin are added to exponentially  
618 growing cells is not too surprising. In contrast, penicillin blocks the TP activity of PBPs, which includes  
619 TP by the bifunctional aPBPs and by the monofunctional bPBPs associated to RodA and FtsW, and thus  
620 all TP activity in the sacculus. However, the effect of sublethal concentrations of penicillin in sacculus  
621 crosslinking within 10 min may not be sufficient to trigger a CESR, or else be compensated by reducing  
622 the activity of PG hydrolases. Bacterial cells are known to be able to accommodate variations in the  
623 amount, the fine composition or the crosslinking of PG, which has been proposed to help to deal with  
624 transient inhibitions of PG synthesis.

625 Finally, lysozyme hydrolyzes the glycosidic linkage between GlcNAc and MurNAc, which can rapidly  
626 compromise the integrity of the sacculus and result in cell lysis. Furthermore, lysozyme directly binds  
627 to the membrane-anchored anti- $\sigma^V$  factor, RsiV, directly inducing  $\sigma^V$  activation and thus the expression  
628 of proteins required for lysozyme resistance [28]. The response to lysozyme is therefore rapidly  
629 detected by CESR systems, but compound-specific rather than a CW damage-triggered response.  
630 Noteworthy, lysozyme and vancomycin show almost inverted induction/repression patterns in their  
631 transcriptional profiles (Fig. 2). The reason for this odd behavior remains to be investigated.

632

633

## 634 **Conclusion**

635 Our comprehensive survey of the primary CESR of *B. subtilis* demonstrates that monitoring (the  
636 inhibition of) the lipid II cycle is the primary check point to monitor the state of PG biosynthesis and  
637 orchestrate adequate countermeasures before lethal damage can occur to the envelope, as has been  
638 thoroughly demonstrated in case of the bacitracin stress response [24, 63, 109]. Our work not only  
639 provides a future reference point for the global transcriptional CESR, it also serves as a direct  
640 comparison of the performance of two profiling approaches – RNAseq vs. tiling arrays – and provides  
641 a collection of highly sensitive whole cell biosensors for monitoring CESR. Such biosensors could be  
642 useful tools in the antibacterial research field. At a time when the spread of bacterial resistance has  
643 become a global threat, the PG cell wall, an essential bacterial structure lacking in higher organisms,  
644 remains the most prominent target for antibacterial therapy [4].

645

## 646 **Materials and Methods**

### 647 **Strains and growth conditions**

648 *Bacillus subtilis* BaSysBio wild type (Nr. 92 in AG Mascher *Bacillus* collection) was used for  
649 transcriptomic study, and routinely grown in Lysogeny Broth (L3522-LB broth, Sigma-Aldrich)  
650 (tryptone, 10 g L<sup>-1</sup>; yeast extract, 5 g L<sup>-1</sup>; NaCl, 10 g L<sup>-1</sup>) at 37 °C with aeration. *B. subtilis* biosensors  
651 were derived from *B. subtilis* W168 (Table S22). *B. subtilis* W168 strains and *E. coli* were routinely  
652 cultivated in LB (Luria/Miller, Carl Roth) (tryptone, 10 g L<sup>-1</sup>; yeast extract, 5 g L<sup>-1</sup>; NaCl, 10 g L<sup>-1</sup>) at 37 °C  
653 with aeration. Solid media contained 1.5% (w/v) agar. Selective media for *B. subtilis* W168 contained  
654 chloramphenicol (5 µg mL<sup>-1</sup>), and for *E. coli* contained ampicillin (100 µg mL<sup>-1</sup>).

### 655 **DNA manipulation and plasmid construction**

656 General cloning procedure, such as PCR, restriction enzyme digestion and ligation, was performed with  
657 enzymes and buffers from New England Biolabs® (NEB, Ipswich, MA, USA) according to respective  
658 protocols. Q5® High-Fidelity DNA polymerase was used for PCRs in case the resulting fragment was  
659 further used, otherwise OneTaq® was the polymerase of choice. PCR purification was performed using  
660 the Hi Yield® PCR Gel Extraction/PCR Clean-up Kit (Süd-Laborbedarf GmbH (SLG), Gauting, Germany).  
661 Plasmid preparation was performed using the Hi Yield® Plasmid Mini-kit. The resulting constructs were  
662 verified by sequencing.

663 To generate promoter-*lux* fusions, the promoters were amplified from the genomic DNA of *B. subtilis*  
664 using respective primer pairs (Table S2424) and cloned into pBS3*Clux*, a reporter vector in the *B. subtilis*  
665 BioBrick Box [110]. The vector and the details of plasmid construction are described in Table S2323.

## 666 ***E. coli* and *B. subtilis* transformation**

667 The chemically competent *E. coli* cells were used for cloning. *E. coli* transformation was done as: 50  $\mu$ L  
668 of *E. coli* competent cells were thawed on ice for about 10 min;  $\frac{1}{2}$  (or the whole) volume of ligation  
669 reaction mix was added to the cells and mixed gently; After 30 min incubation of the tube on ice, the  
670 cells were heat-shocked for 45 seconds at 42 °C and placed back on ice immediately for at least 2 min.  
671 900  $\mu$ L LB medium was added to the tube and incubated at 37 °C for 1 hour with shaking; 50  $\mu$ L or 100  
672  $\mu$ L (depending on experiments) of the recovery culture were plated on selective LB plates and  
673 incubated at 37 °C overnight.

674 *B. subtilis* transformation was performed as: 10 mL MNGE medium was inoculated 1:100 from  
675 overnight cultures of the recipient *B. subtilis* strain. Cultures were grown to OD<sub>600</sub> of 1.1-1.3 at 37 °C,  
676 200 rpm; 400  $\mu$ L of the cells were taken into sterile glass tube for transformation and DNA was added  
677 (2  $\mu$ g linearized plasmid DNA). The mixture was incubated for 1 h at 37 °C with agitation and then 100  
678  $\mu$ L expression mix were added. After another 1 hour of incubation at 37 °C with agitation, 50  $\mu$ L or 100  
679  $\mu$ L (depending on experiments) of the culture were plated on selective LB plates and incubated at 37 °C  
680 overnight. Successful integration of fragment into *B. subtilis* genome was confirmed via colony PCR.

681 MNGE medium: 9.2 mL 1X MN medium (136 g L<sup>-1</sup> dipotassium phosphate x 3 H<sub>2</sub>O, 60 g L<sup>-1</sup>  
682 monopotassium phosphate, and 10 g L<sup>-1</sup> sodium citrate x 2 H<sub>2</sub>O), 1 mL glucose (20%, w/v), 50  $\mu$ L  
683 potassium glutamate (40%, w/v), 50  $\mu$ L ammonium ferric citrate (2.2 mg mL<sup>-1</sup>), 100  $\mu$ L tryptophan (5  
684 mg mL<sup>-1</sup>), and 30  $\mu$ L magnesium sulfate (1 M). Expression mix: 500  $\mu$ L yeast extract (5%, w/v), 250  $\mu$ L  
685 casamino acids (10%, w/v), 50  $\mu$ L tryptophan (5 mg mL<sup>-1</sup>) and 250  $\mu$ L H<sub>2</sub>O.

## 686 **Sample preparation and RNA isolation for RNAseq analyses**

687 The sublethal concentration of the compounds against *B. subtilis* was firstly determined prior to the  
688 induction experiment. The overnight culture was made from fresh single colony of *B. subtilis* grown at  
689 37 °C overnight in a shaker at 200 rpm. 10 mL LB medium in a 100 mL flask was inoculated with  
690 overnight culture by the ratio of 1:100 and incubated at 37 °C with agitation until OD<sub>600</sub> of around 0.4-  
691 0.5 as Day Culture 1. Next, in a 2 L flask, 200 mL LB was inoculated with Day Culture 1 to OD<sub>600</sub> of 0.01  
692 and incubated at 37 °C in a shaker with measurement of OD<sub>600</sub> every 30 min until it reached to ~0.4 as  
693 Day Culture 2. Subsequently, Day Culture 2 was split into fractions of 25 mL in 250 mL flasks, which  
694 were induced with different concentrations of the compounds, leaving one un-induced as control.  
695 OD<sub>600</sub> of each fraction was measured every 30 min up to 2 hours. The concentrations that inhibit *B.*  
696 *subtilis* growth as shown in Fig. S1 (the growth curve at 1  $\mu$ g mL<sup>-1</sup>) were determined as sublethal  
697 concentrations and further applied to induce *B. subtilis* in the following procedure.

698 To prepare bacterial cell samples for RNA isolation, Day Culture 1 and 2 were prepared as described  
699 above. The Day Culture 2 at OD<sub>600</sub> of ~0.4 were split into 25 mL fractions in each pre-warmed 250 mL  
700 flask with an appropriate amount of compounds added already. The cultures were then immediately

701 incubated at 37 °C, 220 rpm. After exact 10 min of induction, the cultures were immediately  
702 transferred into accordingly labeled 50 mL centrifugation tubes (Sarstedt™, Thermo Fisher Scientific)  
703 and put into ice/NaCl bath (ice: NaCl, 3: 1 (v/v)) to efficiently terminate the induction reaction.  
704 Afterwards, the cultures were centrifuged in a precooled centrifuge at 4 °C, 8000 rcf for 2-3 min. The  
705 supernatant was directly decanted from the culture. Cell pellets were then snap-frozen in liquid  
706 nitrogen and stored at -80 °C until use. Every treatment and control samples were made in triplicate.  
707 To isolate total RNA, the *B. subtilis* cell pellets were re-suspended in 200 µL killing buffer (20 mM  
708 Tris/HCl pH 7.5, 5 mM MgCl<sub>2</sub>, 20 mM NaN<sub>3</sub>) and transferred to pre-frozen (in liquid nitrogen)  
709 homogenizer vessel including the steel ball, followed with disruption in a homogenizer (Mikro-  
710 Dismembrator S, Sartorius, Germany) for 2 min at 2600 rom. The cell powder was re-suspended in 4  
711 mL pre-warmed lysis buffer (116.16 g GTC, 2.05 mL sodium acetate (3 M pH 5.2, final conc. 0,025 M),  
712 12.5 mL lauroylsarcosine (10%, final conc. 0.5%), add DEPC-treated H<sub>2</sub>O to 250 mL) and transferred  
713 into four 2 mL reaction tubes with 1 mL in each.

714 1 mL Phenol Mix (Phenol: Chloroform: Isoamylalcohol 25: 24: 1, pH 4.5-5, ROTI® Aqua-P/C/I, for RNA  
715 extraction, Carl Roth, Germany) was added to 1 mL of lysed cells, followed with extraction for 5 min by  
716 vigorous mixing using multi-vortex (Eppendorf). The mixture was centrifuged for 5 min at 12,000 rcf.  
717 Afterwards, around 800 µL supernatant were transferred into a fresh 2 mL reaction tube with 800 µL  
718 Phenol Mix added. A second extraction followed with centrifugation was conducted. Around 700 µL  
719 supernatant were transferred into a fresh 2 mL reaction tube with addition of the same volume of  
720 Chloroform Mix (Chloroform: Isoamylalcohol 24: 1, Roti®-C/I, for nuclear acid extraction, Carl Roth,  
721 Germany). The mixture was extracted and then centrifuged as before. Around 500 µL of the  
722 supernatant were transferred afterwards into a fresh 2 mL reaction tube, followed by the addition of  
723 50 µL (1/10 volume) sodium acetate (3 M, pH 5.2) and 1 mL (2 volume) isopropanol. The mixture was  
724 mixed by inverting and incubate at -80°C overnight. Next day, the precipitation was centrifuged for 30  
725 min at 15,000 rcf, 4 °C in a precooled centrifuge. The supernatant was removed afterwards, and the  
726 pellet was washed twice with 1 mL of 70% ethanol, followed by centrifugation for 5 min at 15,000 rcf,  
727 22 °C. Then, the supernatant was decanted directly and the pellet was dried for about 10 min at room  
728 temperature. After that, the RNA pellet was dissolved in 20-50 µL DEPC treated H<sub>2</sub>O. Two RNA pellets  
729 from one sample were at the end combined into one tube and stored at -80°C until further use.

### 730 **Sample preparation and RNA isolation for tiling array analyses**

731 Overnight cultures of *Bacillus subtilis* wild type strain (grown at 30°C, 200 rpm shaking) were diluted  
732 in fresh medium to OD<sub>600nm</sub> 0.01. Cells were grown at 37°C to mid-exponential phase (OD<sub>600nm</sub> 0.4-0.5),  
733 re-diluted to OD<sub>600nm</sub> 0.01 and further grown at 37°C, 200 rpm until mid-exponential phase.

734 Cultures grown to OD<sub>600nm</sub> 0.4-0.5 were split in 100 mL aliquots for induction with sub-lethal  
735 concentrations of antibiotics, leaving one fraction as uninduced control. After 10 min of incubation at

736 37°C, 35 mL of culture were mixed with 15 mL of ice-cold killing buffer (20 mM Tris/HCl [pH 7.5], 5 mM  
737 MgCl<sub>2</sub>, 20 mM NaN<sub>3</sub>) and immediately centrifuged (5 min, 6000 rpm 4°C). Pellets were frozen in liquid  
738 nitrogen and kept at -80°C.

739 RNA samples were prepared as in Nicolas et al., 2012 with only slight modifications [56]. Briefly, cells  
740 were mechanically lysed by bead beating (Mikro-Dismembrator S from Sartorius) as described  
741 previously. For RNA extraction, 1 volume of acid phenol (Roti-Aqua-phenol from Carl Roth) was mixed  
742 (5 min, 1400 rpm) with 1 volume of cell lysate. Three rounds of extraction with chloroform/isoamyl-  
743 alcohol 24:1 in Tris-HCl [pH 8] were performed before RNA precipitation with 3M sodium acetate and  
744 isopropanol overnight at -20°C. RNA was collected by centrifugation (15000 rpm, 15 min, 4°C), washed  
745 with 70% ethanol, resuspended in 75 µL ddH<sub>2</sub>O and digested with DNaseI (QIAGEN RNase-Free DNase  
746 set (ref. n°79524) for 10 min at RT. Samples were cleaned-up using the Norgen Concentration Micro  
747 Kit (ref. n°23600) according to manufacturer instructions. RNA concentration was determined by  
748 Nanodrop and RNA quality using Agilent Bioanalyzer chip. Hybridization on tiling array chips were realized  
749 at PartnerChip.

#### 750 **Tiling array analysis**

751 Analysis was realized by pooling results from three experiments of each condition. Tiling array data are  
752 obtained with a strand-specific resolution of 22 bp in the different conditions considered in this study.  
753 The analysis used the signal processing and gene-level aggregation procedures used in (P. Nicolas et  
754 al. 2012).

755 Statistical comparison of the 3 biological replicates for each of the considered conditions relied on the  
756 functions “lmFit” and “eBayes” of R package “limma” (Smyth 2004). Control of the False Discovery Rate  
757 relied on q-values obtained with R package “fdrtool” (Strimmer 2008), where the p-values in input are  
758 from “eBayes”. Genes were then considered as differentially expressed if q-values were at least less  
759 than 0.05.

#### 760 **RNA sequencing and analysis**

761 The RNA library quality was verified using LabChip GX Touch HT Nucleic Acid Analyzer. rRNA was  
762 subtracted from the samples with the Illumina Ribo-Zero rRNA removal Kit (Bacteria) according to  
763 manufacturer instructions. The cDNA library was prepared using the NEB Ultra directional RNA library  
764 prep kit for Illumina according to instructions and sequencing was performed on an Illumina HiSeq3000  
765 system. For analysis, the quality of the raw sequencing files was verified using MultiQC. Next, the  
766 sequences were aligned to the *Bacillus subtilis* subsp. *subtilis* str. 168 complete genome (NC\_000964.3)  
767 using Bowtie 2 (Bowtie 2: 2.4.1). Unmapped reads were filtered with Samtools (Samtools: 1.10).  
768 Mapped reads were sorted, and converted to bam file with Samtools (Samtools: 1.10). Gene counts of  
769 aligned reads were quantified using FeatureCounts. The counts were normalized using DESeq2 and a  
770 differential gene expression was calculated (DESeq2: 1.28.0, r-base: 4.0.2). The DESeq 2 comparisons



771 were combined and enriched to an Excel sheet using in-house scripts. Non-treatment condition was  
772 used as the reference point. Genome annotation (in GFF format) was gathered from BSGAtlas (Version  
773 1.0). All raw sequencing data, the processed data files and differential expression data are deposited  
774 at GEO (Gene Expression Omnibus) platform with accession number GSE160345.

775 The hierarchical clustering was performed using Heatmap.2 with in-house scripts and the clustering  
776 was based on the log<sub>2</sub> fold-change value of the 327 genes. The graphs shown in the text were  
777 generated using GraphPad.

### 778 **Luciferase assay**

779 The luciferase activity of *B. subtilis* reporter strains carrying *luxABCDE* operon was assayed using a  
780 Synergy™ NEO multi-mode microplate reader from BioTek® (Winooski, VT, USA). The reader was  
781 controlled by the software Gen5™ (Version 2.06). Luminescence assays were carried out as followed:  
782 10 mL LB medium (w/o antibiotics) were inoculated 1:1000 from overnight cultures (grown with  
783 respective antibiotics) and grown to OD<sub>600</sub> of 0.2-0.3. Then, day cultures were diluted to an OD<sub>600</sub> of  
784 0.01 and 200 µL were transferred into wells of 96-well plate (black wall, clear bottom; Greiner Bio-One,  
785 Frickenhausen, Germany). After one hour of incubation, 5 µL of vancomycin with corresponding  
786 concentrations were added to the culture, respectively. Non-treatment was added with the same  
787 amount of sterile water as the control. The program was set up for incubation of the plate at 37 °C  
788 with agitation (intensity: medium) and the OD<sub>600</sub> as well as the luminescence was recorded every 5 min  
789 for at least 18 hours. Luciferase activity (RLU/OD<sub>600</sub>) was defined as the raw luminescence output  
790 (relative luminescence units, RLU) normalized to OD<sub>600</sub> corrected by medium blank at each time point.

791

### 792 **Acknowledgments**

793 Work in the Carballido-López laboratory was funded by the European Research Council (ERC) under  
794 the European Union's Seventh Framework Program (FP7) and the Horizon 2020 research and  
795 innovation program (grant agreement No 311231 and grant agreement No 772178, respectively, to  
796 R.C.-L.). Work in the Mascher laboratory was supported by grants from the Deutsche  
797 Forschungsgemeinschaft (DFG grant MA2837/3-2) in the framework of the priority program SPP1617  
798 'Phenotypic Heterogeneity and Sociobiology of Bacterial Populations' and the Bundesministerium für  
799 Bildung und Forschung (BMBF) in the framework of the ERAnet Synthetic Biology (project ERASynBio2-  
800 ECFexpress). Q.Z. was supported by the China Scholarship Council and the Graduate Academy of  
801 Technische Universität Dresden.

802

803

## 804 Author contributions

805 T.M and R.C.-L. conceived the study. Q.Z., C.C. and P.F. performed experiments. Q.Z. and C.C. analyzed  
806 the data and generated all figures and tables. C.G., D.M., R.R.M. and V.F. were involved in RNA isolation  
807 and/or analyzing the RNAseq and tiling array experiments. D.W. supervised the experimental work in  
808 the Mascher group. Q.Z. and T.M. wrote the original draft of the manuscript. All authors took part in  
809 the manuscript revision.

810

## 811 References

- 812 1. Dufresne K, Paradis-Bleau C. Biology and Assembly of the Bacterial Envelope. *Adv Exp Med Biol.* 2015;883(41-76).
- 813 2. Silhavy TJ, Kahne D, Walker S. The bacterial cell envelope. *Cold Spring Harb Perspect Biol.* 2010;2(5):a000414.
- 814 3. Angeles DM, Scheffers DJ. The Cell Wall of *Bacillus subtilis*. *Curr Issues Mol Biol.* 2021;41(539-596).
- 815 4. Schneider T, Sahl HG. An oldie but a goodie - cell wall biosynthesis as antibiotic target pathway. *International Journal of Medical Microbiology.* 2010;300(2-3):161-169.
- 816 5. Bugg TD, Braddick D, Dowson CG, Roper DI. Bacterial cell wall assembly: still an attractive antibacterial  
817 target. *Trends Biotechnol.* 2011;29(4):167-173.
- 818 6. Falagas ME, Vouloumanou EK, Samonis G, Vardakas KZ. Fosfomycin. *Clin Microbiol Rev.*  
819 2016;29(2):321-347.
- 820 7. Batson S, de Chiara C, Majce V, Lloyd AJ, Gobec S, Rea D, Fulop V, Thoroughgood CW, Simmons KJ,  
821 Dowson CG, *et al.* Inhibition of D-Ala:D-Ala ligase through a phosphorylated form of the antibiotic D-  
822 cycloserine. *Nat Commun.* 2017;8(1):1939.
- 823 8. Lambert MP, Neuhaus FC. Mechanism of D-cycloserine action: alanine racemase from *Escherichia coli*  
824 W. *J Bacteriol.* 1972;110(3):978-987.
- 825 9. Neuhaus FC, Lynch JL. The Enzymatic Synthesis of D-Alanyl-D-Alanine. 3. On the Inhibition of D-Alanyl-  
826 D-Alanine Synthetase by the Antibiotic D-Cycloserine. *Biochemistry.* 1964;3(471-480).
- 827 10. Takatsuki A, Arima K, Tamura G. Tunicamycin, a new antibiotic. I Isolation and characterization of  
828 tunicamycin. *J Antibiot (Tokyo).* 1971;24(4):215-223.
- 829 11. Bugg TD, Lloyd AJ, Roper DI. Phospho-MurNAc-pentapeptide translocase (MraY) as a target for  
830 antibacterial agents and antibacterial proteins. *Infect Disord Drug Targets.* 2006;6(2):85-106.
- 831 12. Mirouze N, Ferret C, Cornilleau C, Carballido-López R. Antibiotic sensitivity reveals that wall teichoic  
832 acids mediate DNA binding during competence in *Bacillus subtilis*. *Nat Commun.* 2018;9(1):5072.
- 833 13. Brandish PE, Burnham MK, Lonsdale JT, Southgate R, Inukai M, Bugg TD. Slow binding inhibition of  
834 phospho-N-acetylmuramyl-pentapeptide-translocase (*Escherichia coli*) by mureidomycin A. *J Biol*  
835 *Chem.* 1996;271(13):7609-7614.
- 836 14. Campbell J, Singh AK, Santa Maria JP, Jr., Kim Y, Brown S, Swoboda JG, Mylonakis E, Wilkinson BJ,  
837 Walker S. Synthetic lethal compound combinations reveal a fundamental connection between wall  
838 teichoic acid and peptidoglycan biosyntheses in *Staphylococcus aureus*. *ACS Chem Biol.* 2011;6(1):106-  
839 116.
- 840 15. Azevedo EC, Rios EM, Fukushima K, Campos-Takaki GM. Bacitracin production by a new strain of  
841 *Bacillus subtilis*. *Appl Biochem Biotechnol.* 1993;42(1):1-7.
- 842 16. Stone KJ, Strominger JL. Mechanism of action of bacitracin: complexation with metal ion and C 55 -  
843 isoprenyl pyrophosphate. *Proceedings of the National Academy of Sciences.* 1971;68(12):3223-3227.
- 844 17. Storm DR, Strominger JL. Complex formation between bacitracin peptides and isoprenyl  
845 pyrophosphates: The specificity of lipid-peptide interactions. *Journal of Biological Chemistry.*  
846 1973;248(11):3940-3945.
- 847 18. Kahne D, Leimkuhler C, Lu W, Walsh C. Glycopeptide and lipoglycopeptide antibiotics. *Chem Rev.*  
848 2005;105(2):425-448.
- 849 19. Ostash B, Doud E, Fedorenko V. The molecular biology of moenomycins: towards novel antibiotics  
850 based on inhibition of bacterial peptidoglycan glycosyltransferases. *Biol Chem.* 2010;391(5):499-504.
- 851
- 852
- 853

- 854 20. Ostash B, Walker S. Moenomycin family antibiotics: chemical synthesis, biosynthesis, and biological  
855 activity. *Nat Prod Rep*. 2010;27(11):1594-1617.
- 856 21. Strominger JL, Tipper DJ. Bacterial cell wall synthesis and structure in relation to the mechanism of  
857 action of penicillins and other antibacterial agents. *Am J Med*. 1965;39(5):708-721.
- 858 22. Chipman DM, Sharon N. Mechanism of lysozyme action. *Science*. 1969;165(3892):454-465.
- 859 23. Jordan S, Hutchings MI, Mascher T. Cell envelope stress response in Gram-positive bacteria. *FEMS*  
860 *Microbiol Rev*. 2008;32(1):107-146.
- 861 24. Radeck J, Fritz G, Mascher T. The cell envelope stress response of *Bacillus subtilis*: from static signaling  
862 devices to dynamic regulatory network. *Current Genetics*. 2017;63(1):79-90.
- 863 25. Helmann JD. *Bacillus subtilis* extracytoplasmic function (ECF) sigma factors and defense of the cell  
864 envelope. *Curr Opin Microbiol*. 2016;30(122-132).
- 865 26. Helmann JD. Deciphering a complex genetic regulatory network: the *Bacillus subtilis*  $\sigma^W$  protein and  
866 intrinsic resistance to antimicrobial compounds. *Sci Prog*. 2006;89(Pt 3-4):243-266.
- 867 27. Cao M, Helmann JD. The *Bacillus subtilis* extracytoplasmic-function  $\sigma^X$  factor regulates modification of  
868 the cell envelope and resistance to cationic antimicrobial peptides. *J Bacteriol*. 2004;186(4):1136-  
869 1146.
- 870 28. Ho TD, Ellermeier CD. Activation of the extracytoplasmic function sigma factor  $\sigma^V$  by lysozyme.  
871 *Molecular Microbiology*. 2019;112(2):410-419.
- 872 29. Schrecke K, Staroń A, Mascher T. Two-component signaling in the Gram-positive envelope stress  
873 response: intramembrane-sensing histidine kinases and accessory membrane proteins. In *Two*  
874 *component systems in bacteria*. Edited by Gross R, Beier D. Hethersett, Norwich, UK: Horizon Scientific  
875 Press; 2012:in press.
- 876 30. Mascher T, Zimmer SL, Smith TA, Helmann JD. Antibiotic-inducible promoter regulated by the cell  
877 envelope stress-sensing two-component system LiaRS of *Bacillus subtilis*. *Antimicrob Agents*  
878 *Chemother*. 2004;48(8):2888-2896.
- 879 31. Müller A, Wenzel M, Strahl H, Grein F, Saaki TNV, Kohl B, Siersma T, Bandow JE, Sahl HG, Schneider T,  
880 Hamoen LW. Daptomycin inhibits cell envelope synthesis by interfering with fluid membrane  
881 microdomains. *Proceedings of the National Academy of Sciences*. 2016;113(45):E7077-E7086.
- 882 32. Wecke T, Zühlke D, Mäder U, Jordan S, Voigt B, Pelzer S, Labischinski H, Homuth G, Hecker M, Mascher  
883 T. Daptomycin versus Friulimycin B: in-depth profiling of *Bacillus subtilis* cell envelope stress responses.  
884 *Antimicrob Agents Chemother*. 2009;53(4):1619-1623.
- 885 33. Dintner S, Staroń A, Berchtold E, Petri T, Mascher T, Gebhard S. Coevolution of ABC transporters and  
886 two-component regulatory systems as resistance modules against antimicrobial peptides in *Firmicutes*  
887 *Bacteria*. *J Bacteriol*. 2011;193(15):3851-3862.
- 888 34. Piepenbreier H, Fritz G, Gebhard S. Transporters as information processors in bacterial signalling  
889 pathways. *Mol Microbiol*. 2017;104(1):1-15.
- 890 35. Revilla-Guarinos A, Gebhard S, Mascher T, Zúñiga M. Defence against antimicrobial peptides: different  
891 strategies in *Firmicutes*. *Environ Microbiol*. 2014;16(5):1225-1237.
- 892 36. Staroń A, Finkeisen DE, Mascher T. Peptide antibiotic sensing and detoxification modules of *Bacillus*  
893 *subtilis*. *Antimicrob Agents Chemother*. 2011;55(2):515-525.
- 894 37. Westers H, Westers L, Darmon E, van Dijl JM, Quax WJ, Zanen G. The CsaRS two-component regulatory  
895 system controls a general secretion stress response in *Bacillus subtilis*. *FEBS J*. 2006;273(16):3816-  
896 3827.
- 897 38. Neef J, Bongiorno C, Schmidt B, Goosens VJ, van Dijl JM. Relative contributions of non-essential Sec  
898 pathway components and cell envelope-associated proteases to high-level enzyme secretion by  
899 *Bacillus subtilis*. *Microb Cell Fact*. 2020;19(1):52.
- 900 39. Dubrac S, Bisicchia P, Devine KM, Msadek T. A matter of life and death: cell wall homeostasis and the  
901 WalkR (YycGF) essential signal transduction pathway. *Mol Microbiol*. 2008;70(6):1307-1322.
- 902 40. Dubrac S, Boneca IG, Poupel O, Msadek T. New insights into the Walk/WalR (YycG/YycF) essential  
903 signal transduction pathway reveal a major role in controlling cell wall metabolism and biofilm  
904 formation in *Staphylococcus aureus*. *J Bacteriol*. 2007;189(22):8257-8269.
- 905 41. Fabret C, Hoch JA. A two-component signal transduction system essential for growth of *Bacillus*  
906 *subtilis*: implications for anti-infective therapy. *J Bacteriol*. 1998;180(23):6375-6383.
- 907 42. Wagner C, Saizieu Ad A, Schönfeld HJ, Kamber M, Lange R, Thompson CJ, Page MG. Genetic analysis  
908 and functional characterization of the *Streptococcus pneumoniae* vic operon. *Infect Immun*.  
909 2002;70(11):6121-6128.
- 910 43. Takada H, Yoshikawa H. Essentiality and function of Walk/WalR two-component system: the past,  
911 present, and future of research. *Biosci Biotechnol Biochem*. 2018;82(5):741-751.

- 912 44. Salzberg LI, Powell L, Hokamp K, Botella E, Noone D, Devine KM. The WalRK (YycFG) and  $\sigma^I$  RsgI  
913 regulators cooperate to control CwlO and LytE expression in exponentially growing and stressed  
914 *Bacillus subtilis* cells. *Mol Microbiol.* 2013;87(1):180-195.
- 915 45. Bisicchia P, Noone D, Lioliou E, Howell A, Quigley S, Jensen T, Jarmer H, Devine KM. The essential  
916 YycFG two-component system controls cell wall metabolism in *Bacillus subtilis*. *Mol Microbiol.*  
917 2007;65(1):180-200.
- 918 46. Dobihal GS, Brunet YR, Flores-Kim J, Rudner DZ. Homeostatic control of cell wall hydrolysis by the  
919 WalRK two-component signaling pathway in *Bacillus subtilis*. *Elife.* 2019;8(
- 920 47. Haeusser DP, Margolin W. Splitsville: structural and functional insights into the dynamic bacterial Z  
921 ring. *Nature Reviews Microbiology.* 2016;14(5):305-319.
- 922 48. Fukuchi K, Kasahara Y, Asai K, Kobayashi K, Moriya S, Ogasawara N. The essential two-component  
923 regulatory system encoded by *yycF* and *yycG* modulates expression of the *ftsAZ* operon in *Bacillus*  
924 *subtilis*. *Microbiology.* 2000;146(7):1573-1583.
- 925 49. Grifoll-Romero L, Sainz-Polo MA, Albesa-Jové D, Guerin ME, Biarnés X, Planas A. Structure-function  
926 relationships underlying the dual *N*-acetylmuramic and *N*-acetylglucosamine specificities of the  
927 bacterial peptidoglycan deacetylase PdaC. *Journal of Biological Chemistry.* 2019;294(50):19066-19080.
- 928 50. Salzberg LI, Helmann JD. An antibiotic-inducible cell wall-associated protein that protects *Bacillus*  
929 *subtilis* from autolysis. *J Bacteriol.* 2007;189(13):4671-4680.
- 930 51. Wecke T, Mascher T. Antibiotic research in the age of omics: from expression profiles to interspecies  
931 communication. *J Antimicrob Chemother.* 2011;66(12):2689-2704.
- 932 52. Cao M, Wang T, Ye R, Helmann JD. Antibiotics that inhibit cell wall biosynthesis induce expression of  
933 the *Bacillus subtilis*  $\sigma^W$  and  $\sigma^M$  regulons. *Mol Microbiol.* 2002;45(5):1267-1276.
- 934 53. Mascher T, Margulis NG, Wang T, Ye RW, Helmann JD. Cell wall stress responses in *Bacillus subtilis*: the  
935 regulatory network of the bacitracin stimulon. *Mol Microbiol.* 2003;50(5):1591-1604.
- 936 54. Kunst F, Ogasawara N, Moszer I, Albertini AM, Alloni G, Azevedo V, Bertero MG, Bessières P, Bolotin A,  
937 Borchert S, *et al.* The complete genome sequence of the gram-positive bacterium *Bacillus subtilis*.  
938 *Nature.* 1997;390(6657):249-256.
- 939 55. Barbe V, Cruveiller S, Kunst F, Lenoble P, Meurice G, Sekowska A, Vallenet D, Wang T, Moszer I,  
940 Medigue C, Danchin A. From a consortium sequence to a unified sequence: the *Bacillus subtilis* 168  
941 reference genome a decade later. *Microbiology.* 2009;155(6):1758-1775.
- 942 56. Nicolas P, Mäder U, Dervyn E, Rochat T, Leduc A, Pigeonneau N, Bidnenko E, Marchadier E, Hoebeke  
943 M, Aymerich S, *et al.* Condition-dependent transcriptome reveals high-level regulatory architecture in  
944 *Bacillus subtilis*. *Science.* 2012;335(6072):1103-1106.
- 945 57. Geissler AS, Anthon C, Alkan F, Gonzalez-Tortuero E, Poulsen LD, Kallehauge TB, Breuner A, Seemann  
946 SE, Vinther J, Gorodkin J. BSGAtlas: a unified *Bacillus subtilis* genome and transcriptome annotation  
947 atlas with enhanced information access. *Microb Genom.* 2021;7(2).
- 948 58. Pedreira T, Elfmann C, Stulke J. The current state of SubtiWiki, the database for the model organism  
949 *Bacillus subtilis*. *Nucleic Acids Res.* 2022;50(D1):D875-D882.
- 950 59. Hakulinen JK, Hering J, Brändén G, Chen H, Snijder A, Ek M, Johansson P. MraY-antibiotic complex  
951 reveals details of tunicamycin mode of action. *Nat Chem Biol.* 2017;13(3):265-267.
- 952 60. Cao M, Helmann JD. Regulation of the *Bacillus subtilis* *bcrC* bacitracin resistance gene by two  
953 extracytoplasmic function  $\sigma$  factors. *J Bacteriol.* 2002;184(22):6123-6129.
- 954 61. Pooley HM, Karamata D. Incorporation of [2-<sup>3</sup>H]glycerol into cell surface components of *Bacillus*  
955 *subtilis* 168 and thermosensitive mutants affected in wall teichoic acid synthesis: effect of  
956 tunicamycin. *Microbiology.* 2000;146 ( Pt 4)(797-805.
- 957 62. Ohki R, Giyanto, Tateno K, Masuyama W, Moriya S, Kobayashi K, Ogasawara N. The BceRS two-  
958 component regulatory system induces expression of the bacitracin transporter, BceAB, in *Bacillus*  
959 *subtilis*. *Mol Microbiol.* 2003;49(4):1135-1144.
- 960 63. Radeck J, Gebhard S, Orchard PS, Kirchner M, Bauer S, Mascher T, Fritz G. Anatomy of the bacitracin  
961 resistance network in *Bacillus subtilis*. *Mol Microbiol.* 2016;100(4):607-620.
- 962 64. Adler RH, Snoke JE. Requirement of divalent metal ions for bacitracin activity. *J Bacteriol.*  
963 1962;83(1315-1317.
- 964 65. Moore CM, Gaballa A, Hui M, Ye RW, Helmann JD. Genetic and physiological responses of *Bacillus*  
965 *subtilis* to metal ion stress. *Mol Microbiol.* 2005;57(1):27-40.
- 966 66. Hecker M, Pané-Farré J, Volker U. SigB-dependent general stress response in *Bacillus subtilis* and  
967 related gram-positive bacteria. *Annu Rev Microbiol.* 2007;61(215-236.
- 968 67. Salzberg LI, Luo Y, Hachmann AB, Mascher T, Helmann JD. The *Bacillus subtilis* GntR family repressor  
969 YtrA responds to cell wall antibiotics. *J Bacteriol.* 2011;193(20):5793-5801.

- 970 68. Guariglia-Oropeza V. Cell envelope stress response and antimicrobial resistance in *Bacillus subtilis*.  
971 Cornell University 2013.
- 972 69. Hutter B, Schaab C, Albrecht S, Borgmann M, Brunner NA, Freiberg C, Ziegelbauer K, Rock CO, Ivanov I,  
973 Loferer H. Prediction of mechanisms of action of antibacterial compounds by gene expression  
974 profiling. *Antimicrob Agents Chemother*. 2004;48(8):2838-2844.
- 975 70. Callewaert L, Michiels CW. Lysozymes in the animal kingdom. *J Biosci*. 2010;35(1):127-160.
- 976 71. Guariglia-Oropeza V, Helmann JD. *Bacillus subtilis*  $\sigma^V$  confers lysozyme resistance by activation of two  
977 cell wall modification pathways, peptidoglycan O-acetylation and D-alanylation of teichoic acids. *J*  
978 *Bacteriol*. 2011;193(22):6223-6232.
- 979 72. Ho TD, Hastie JL, Intile PJ, Ellermeier CD. The *Bacillus subtilis* extracytoplasmic function  $\sigma$  factor  $\sigma^V$  is  
980 induced by lysozyme and provides resistance to lysozyme. *J Bacteriol*. 2011;193(22):6215-6222.
- 981 73. Doan T, Servant P, Tojo S, Yamaguchi H, Lerondel G, Yoshida KI, Fujita Y, Aymerich S. The *Bacillus*  
982 *subtilis* *ywka* gene encodes a malic enzyme and its transcription is activated by the YufL/YufM two-  
983 component system in response to malate. *Microbiology (Reading)*. 2003;149(Pt 9):2331-2343.
- 984 74. Eiamphungporn W, Helmann JD. The *Bacillus subtilis*  $\sigma^M$  regulon and its contribution to cell envelope  
985 stress responses. *Mol Microbiol*. 2008;67(4):830-848.
- 986 75. Cao M, Kobel PA, Morshedi MM, Wu MF, Paddon C, Helmann JD. Defining the *Bacillus subtilis*  $\sigma^W$   
987 regulon: a comparative analysis of promoter consensus search, run-off transcription/microarray  
988 analysis (ROMA), and transcriptional profiling approaches. *J Mol Biol*. 2002;316(3):443-457.
- 989 76. Huang X, Fredrick KL, Helmann JD. Promoter recognition by *Bacillus subtilis*  $\sigma^W$ : autoregulation and  
990 partial overlap with the  $\sigma^X$  regulon. *J Bacteriol*. 1998;180(15):3765-3770.
- 991 77. Zellmeier S, Hofmann C, Thomas S, Wiegert T, Schumann W. Identification of  $\sigma^V$ -dependent genes of  
992 *Bacillus subtilis*. *FEMS Microbiol Lett*. 2005;253(2):221-229.
- 993 78. Helmann JD. The extracytoplasmic function (ECF) sigma factors. *Adv Microb Physiol*. 2002;46(47-110).
- 994 79. Mascher T, Hachmann AB, Helmann JD. Regulatory overlap and functional redundancy among *Bacillus*  
995 *subtilis* extracytoplasmic function  $\sigma$  factors. *J Bacteriol*. 2007;189(19):6919-6927.
- 996 80. Zweers JC, Nicolas P, Wiegert T, van Dijl JM, Denham EL. Definition of the  $\sigma^W$  regulon of *Bacillus subtilis*  
997 in the absence of stress. *PLoS One*. 2012;7(11):e48471.
- 998 81. Asai K, Yamaguchi H, Kang CM, Yoshida K, Fujita Y, Sadaie Y. DNA microarray analysis of *Bacillus subtilis*  
999 sigma factors of extracytoplasmic function family. *FEMS Microbiol Lett*. 2003;220(1):155-160.
- 1000 82. Petersohn A, Brigulla M, Haas S, Hoheisel JD, Völker U, Hecker M. Global analysis of the general stress  
1001 response of *Bacillus subtilis*. *J Bacteriol*. 2001;183(19):5617-5631.
- 1002 83. Mascher T, Zimmer SL, Smith TA, Helmann JD. Antibiotic-inducible promoter regulated by the cell  
1003 envelope stress-sensing two-component system LiaRS of *Bacillus subtilis*. *Antimicrob Agents*  
1004 *Chemother*. 2004;48(8):2888-2896.
- 1005 84. Wolf D, Kalamorz F, Wecke T, Juszczak A, Mäder U, Homuth G, Jordan S, Kirstein J, Hoppert M, Voigt B,  
1006 *et al*. In-depth profiling of the LiaR response of *Bacillus subtilis*. *J Bacteriol*. 2010;192(18):4680-4693.
- 1007 85. Jordan S, Junker A, Helmann JD, Mascher T. Regulation of LiaRS-dependent gene expression in *Bacillus*  
1008 *subtilis*: identification of inhibitor proteins, regulator binding sites, and target genes of a conserved cell  
1009 envelope stress-sensing two-component system. *J Bacteriol*. 2006;188(14):5153-5166.
- 1010 86. Kobras CM, Piepenbreier H, Emenegger J, Sim A, Fritz G, Gebhard S. BceAB-Type Antibiotic Resistance  
1011 Transporters Appear To Act by Target Protection of Cell Wall Synthesis. *Antimicrob Agents Chemother*.  
1012 2020;64(3):e02241-02219.
- 1013 87. Rietkötter E, Hoyer D, Mascher T. Bacitracin sensing in *Bacillus subtilis*. *Mol Microbiol*. 2008;68(3):768-  
1014 785.
- 1015 88. Pietiäinen M, Gardemeister M, Mecklin M, Leskelä S, Sarvas M, Kontinen VP. Cationic antimicrobial  
1016 peptides elicit a complex stress response in *Bacillus subtilis* that involves ECF-type sigma factors and  
1017 two-component signal transduction systems. *Microbiology*. 2005;151(Pt 5):1577-1592.
- 1018 89. Müller A, Wolf D, Gutzeit HO. The black soldier fly, *Hermetia illucens* - a promising source for  
1019 sustainable production of proteins, lipids and bioactive substances. *Zeitschrift für Naturforschung C*.  
1020 2017;72(9-10):351-363.
- 1021 90. Meisner J, Montero Llopis P, Sham LT, Garner E, Bernhardt TG, Rudner DZ. FtsEX is required for CwlO  
1022 peptidoglycan hydrolase activity during cell wall elongation in *Bacillus subtilis*. *Mol Microbiol*.  
1023 2013;89(6):1069-1083.
- 1024 91. Kobayashi K, Sudiarta IP, Kodama T, Fukushima T, Ara K, Ozaki K, Sekiguchi J. Identification and  
1025 characterization of a novel polysaccharide deacetylase C (PdaC) from *Bacillus subtilis*. *Journal of*  
1026 *Biological Chemistry*. 2012;287(13):9765-9776.

- 1027 92. Wolf D, Mascher T. The applied side of antimicrobial peptide-inducible promoters from *Firmicutes*  
1028 bacteria: expression systems and whole-cell biosensors. *Appl Microbiol Biotechnol.*  
1029 2016;100(11):4817-4829.
- 1030 93. Kobras CM, Mascher T, Gebhard S. Application of a *Bacillus subtilis* Whole-Cell Biosensor (*P<sub>liaI</sub>-lux*) for  
1031 the Identification of Cell Wall Active Antibacterial Compounds. In *Antibiotics* (Basel). Humana Press,  
1032 New York, NY; 2017:121-131.
- 1033 94. Zielińska A, Savietto A, de Sousa Borges A, Martinez D, Berbon M, Roelofsen JR, Hartman AM, de Boer  
1034 R, Van der Klei IJ, Hirsch AK, *et al.* Flotillin-mediated membrane fluidity controls peptidoglycan  
1035 synthesis and MreB movement. *Elife.* 2020;9(e57179).
- 1036 95. Miyamoto T, Katane M, Saitoh Y, Sekine M, Homma H. Identification and characterization of novel  
1037 broad-spectrum amino acid racemases from *Escherichia coli* and *Bacillus subtilis*. *Amino Acids.*  
1038 2017;49(11):1885-1894.
- 1039 96. Popp PF, Gumerov VM, Andrianova EP, Bewersdorf L, Mascher T, Joulina I, Wolf D. Phyletic  
1040 distribution and diversification of the Phage Shock Protein stress response system in bacteria and  
1041 archaea. *bioRxiv.* 2021:<https://doi.org/10.1101/2021.1102.1115.431232>.
- 1042 97. Cao M, Bernat BA, Wang Z, Armstrong RN, Helmann JD. FosB, a cysteine-dependent fosfomycin  
1043 resistance protein under the control of  $\sigma^W$ , an extracytoplasmic-function  $\sigma$  factor in *Bacillus subtilis*. *J*  
1044 *Bacteriol.* 2001;183(7):2380-2383.
- 1045 98. Palmer CN, Gustafsson MC, Dobson H, von Wachenfeldt C, Wolf CR. Adaptive responses to fatty acids  
1046 are mediated by the regulated expression of cytochromes P450. *Biochem Soc Trans.* 1999;27(4):374-  
1047 378.
- 1048 99. Hutter B, Fischer C, Jacobi A, Schaab C, Loferer H. Panel of *Bacillus subtilis* reporter strains indicative of  
1049 various modes of action. *Antimicrob Agents Chemother.* 2004;48(7):2588-2594.
- 1050 100. Schneider T, Kruse T, Wimmer R, Wiedemann I, Sass V, Pag U, Jansen A, Nielsen AK, Mygind PH,  
1051 Raventós DS, *et al.* Plectasin, a fungal defensin, targets the bacterial cell wall precursor Lipid II.  
1052 *Science.* 2010;328(5982):1168-1172.
- 1053 101. Culp EJ, Waglechner N, Wang W, Fiebig-Comyn AA, Hsu YP, Koteva K, Sychantha D, Coombes BK, Van  
1054 Nieuwenhze MS, Brun YV, Wright GD. Evolution-guided discovery of antibiotics that inhibit  
1055 peptidoglycan remodelling. *Nature.* 2020;578(7796):582-587.
- 1056 102. Czarny TL, Perri AL, French S, Brown ED. Discovery of novel cell wall-active compounds using P ywaC, a  
1057 sensitive reporter of cell wall stress, in the model gram-positive bacterium *Bacillus subtilis*. *Antimicrob*  
1058 *Agents Chemother.* 2014;58(6):3261-3269.
- 1059 103. Nicolas P, Mäder U, Dervyn E, Rochat T, Leduc A, Pigeonneau N, Bidnenko E, Marchadier E, Hoebeke  
1060 M, Aymerich S, *et al.* Condition-dependent transcriptome reveals high-level regulatory architecture in  
1061 *Bacillus subtilis*. *Science.* 2012;335(6072):1103-1106.
- 1062 104. Jordan S, Hutchings MI, Mascher T. Cell envelope stress response in Gram-positive bacteria. *FEMS*  
1063 *Microbiol Rev.* 2008;32(1):107-146.
- 1064 105. Typas A, Banzhaf M, Gross CA, Vollmer W. From the regulation of peptidoglycan synthesis to bacterial  
1065 growth and morphology. *Nat Rev Microbiol.* 2011;10(2):123-136.
- 1066 106. Carballido-Lopez R, Formstone A. Shape determination in *Bacillus subtilis*. *Curr Opin Microbiol.*  
1067 2007;10(6):611-616.
- 1068 107. Cho H, Wivagg CN, Kapoor M, Barry Z, Rohs PDA, Suh H, Marto JA, Garner EC, Bernhardt TG. Bacterial  
1069 cell wall biogenesis is mediated by SEDS and PBP polymerase families functioning semi-autonomously.  
1070 *Nat Microbiol.* 2016;1(16172).
- 1071 108. McPherson DC, Popham DL. Peptidoglycan synthesis in the absence of class A penicillin-binding  
1072 proteins in *Bacillus subtilis*. *J Bacteriol.* 2003;185(4):1423-1431.
- 1073 109. Piepenbreier H, Sim A, Kobras CM, Radeck J, Mascher T, Gebhard S, Fritz G. From Modules to  
1074 Networks: a Systems-Level Analysis of the Bacitracin Stress Response in *Bacillus subtilis*. *mSystems.*  
1075 2020;5(1).
- 1076 110. Radeck J, Kraft K, Bartels J, Cikovic T, Dürr F, Emenegger J, Kelterborn S, Sauer C, Fritz G, Gebhard S,  
1077 Mascher T. The *Bacillus* BioBrick Box: generation and evaluation of essential genetic building blocks for  
1078 standardized work with *Bacillus subtilis*. *J Biol Eng.* 2013;7(1):1-17.

1079  
1080

## 1081 List of figures, tables and supplemental material

1082

1083 Fig. 1 The peptidoglycan biosynthetic pathway showing sites of action of the compounds applied in the study.

1084 Fig. 2 Hierarchical clustering analysis of the transcriptional profiles of *B. subtilis* in response to cell envelope-  
1085 active compounds.

1086 Fig. 3 Graphic presentation of the stimulons.

1087 Fig. 4 Induction profiles of *sigW*, *sigM*, *sigV* and *sigX* by the CESs.

1088 Fig. 5 Transcriptional response of two-component systems under cell envelope stresses.

1089 Fig. 6 Transcriptional response of WalR regulon to cell envelope-active compounds.

1090 Fig. 7 Vancomycin stimulon (RNAseq vs Tiling array).

1091 Fig. 8 Expression patterns of CESR marker genes.

1092 Fig. 9 Dose-dependent response of *B. subtilis* biosensors to vancomycin.

1093

1094 Fig. S1 Effect of treatment of different concentrations of vancomycin on *B. subtilis* growth.

1095 Fig. S2 Transcriptional response of rRNA-coding gene to different CESs.

1096 Fig. S3 Hierarchical clustering analysis of the transcriptional profiles of *B. subtilis* in response to cell envelope-  
1097 active compounds (tiling array).

1098 Fig. S4 Clustering analysis of the ECF sigma regulons.

1099 Fig. S5 Promoter consensus sequences.

1100 Fig. S6 Dose-response of *B. subtilis* biosensors to vancomycin.

1101 Fig. S7 Dose-response of *B. subtilis* biosensor with promoter  $P_{iseA}$  to penicillin G.

1102 Fig. S8 Induction of *B. subtilis* biosensors to bacitracin and/or moenomycin.

1103

1104 Table 1 Top 5 differentially expressed genes in each of the stimulons.

1105 Table 2 Overview of ECF  $\sigma^M$ ,  $\sigma^W$ ,  $\sigma^X$  and  $\sigma^V$  regulons (RNAseq & Tiling array).

1106

1107 Table S1 Complete table of differentially expressed genes with RNAseq.

1108 Table S2 Complete table of differentially expressed genes with tiling array.

1109 Table S3 The full list of genes applied to generate heatmap with the corresponding clusters assigned marked.

1110 Table S4 Genes induced or repressed ( $\geq 2$  fold) in fosfomycin stimulon with RNAseq.

1111 Table S5 Genes induced or repressed ( $\geq 2$  fold) in fosfomycin stimulon with tiling array.

1112 Table S6 Genes induced or repressed ( $\geq 2$  fold) in D-cycloserine stimulon with RNAseq.

1113 Table S7 Genes induced or repressed ( $\geq 2$  fold) in D-cycloserine stimulon with tiling array.

1114 Table S8 Genes induced or repressed ( $\geq 5$  fold) in tunicamycin stimulon with RNAseq.

1115 Table S9 Genes induced or repressed ( $\geq 5$  fold) in tunicamycin stimulon with tiling array.

1116 Table S10 Genes induced or repressed ( $\geq 5$  fold) in bacitracin stimulon with RNAseq.

1117 Table S11 Genes induced or repressed ( $\geq 5$  fold) in bacitracin stimulon with tiling array.

1118 Table S12 Genes induced or repressed ( $\geq 5$  fold) in vancomycin stimulon with RNAseq.

- 1119 Table S13 Genes induced or repressed ( $\geq 5$  fold) in vancomycin stimulon with tiling array.
- 1120 Table S14 Genes induced or repressed ( $\geq 2$  fold) in moenomycin stimulon with RNAseq.
- 1121 Table S15 Genes induced or repressed ( $\geq 2$  fold) in moenomycin stimulon with tiling array.
- 1122 Table S16 Genes induced or repressed ( $\geq 2$  fold) in penicillin G stimulon with RNAseq.
- 1123 Table S17 Genes induced or repressed ( $\geq 2$  fold) in penicillin G stimulon with tiling array.
- 1124 Table S18 Genes induced or repressed ( $\geq 5$  fold) in lysozyme stimulon with RNAseq.
- 1125 Table S19 Genes induced or repressed ( $\geq 5$  fold) in lysozyme stimulon with tiling array.
- 1126 Table S20 Genes for clustering analysis of ECF sigma regulons.
- 1127 Table S21 New features significant in at least one condition of RNAseq and tiling array.
- 1128 Table S22 Bacterial strains used in this study.
- 1129 Table S23 Vector and plasmids used in this study.
- 1130 Table S24 Oligonucleotides used in this study.



# Comprehensive and Comparative Transcriptional Profiling of the Cell Wall Stress Response in *Bacillus subtilis*

Qian Zhang<sup>1#</sup>, Charlene Cornilleau<sup>2#</sup>, Raphael R. Müller<sup>3</sup>, Doreen Meier<sup>4</sup>, Pierre Flores<sup>2</sup>, Cyprien Guérin<sup>5</sup>, Diana Wolf<sup>1</sup>, Vincent Fromion<sup>2</sup>, Rut Carballido-Lopez<sup>2§</sup>,  
and Thorsten Mascher<sup>1§</sup>†

<sup>1</sup> Technische Universität (TU) Dresden, Institute of Microbiology, Germany

<sup>2</sup> MICALIS Institute, INRAE, AgroParisTech, Université Paris-Saclay, 78350 Jouy-en-Josas, France

<sup>3</sup> Bioinformatics and Systems Biology, Justus-Liebig-Universität, Gießen, Germany

<sup>4</sup> SYNMIKRO and Philipps-Universität Marburg, Germany

<sup>5</sup> MaIAGE, INRAE, Université Paris-Saclay, 78350 Jouy-en-Josas, France.

# These two authors contributed equally to this work

§ Authors for correspondence:

[thorsten.mascher@tu-dresden.de](mailto:thorsten.mascher@tu-dresden.de), [rut.carballido-lopez@inrae.fr](mailto:rut.carballido-lopez@inrae.fr)

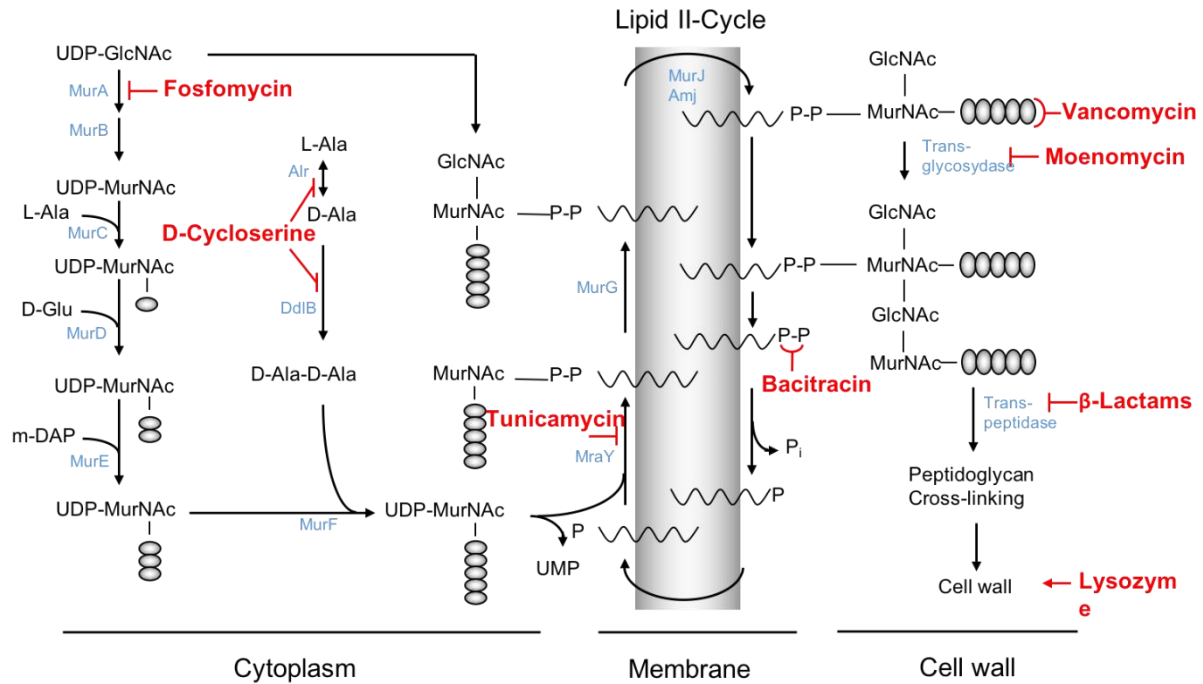


Fig. 1 The peptidoglycan biosynthetic pathway showing sites of action of the compounds applied in the study. The pathway involves three stages as described in the main text. Cell envelope-active compounds applied in this study are given and placed next to the steps they inhibit. Some of the enzymes involved in the cell wall biosynthesis are shown in light blue next to the corresponding catalytic steps. Lipid II is the GlcNAc-MurNAc-pentapeptide covalently linked to the lipid carrier undecaprenol (symbolized by the wavy lines) via pyrophosphate ester bridge. Abbreviation: GlcNAc, N-acetyl-glucosamine; MurNAc, N-acetyl-muramic acid. Amino acids are symbolized by small grey circles. This figure was generated based on (2, 3) with modifications.

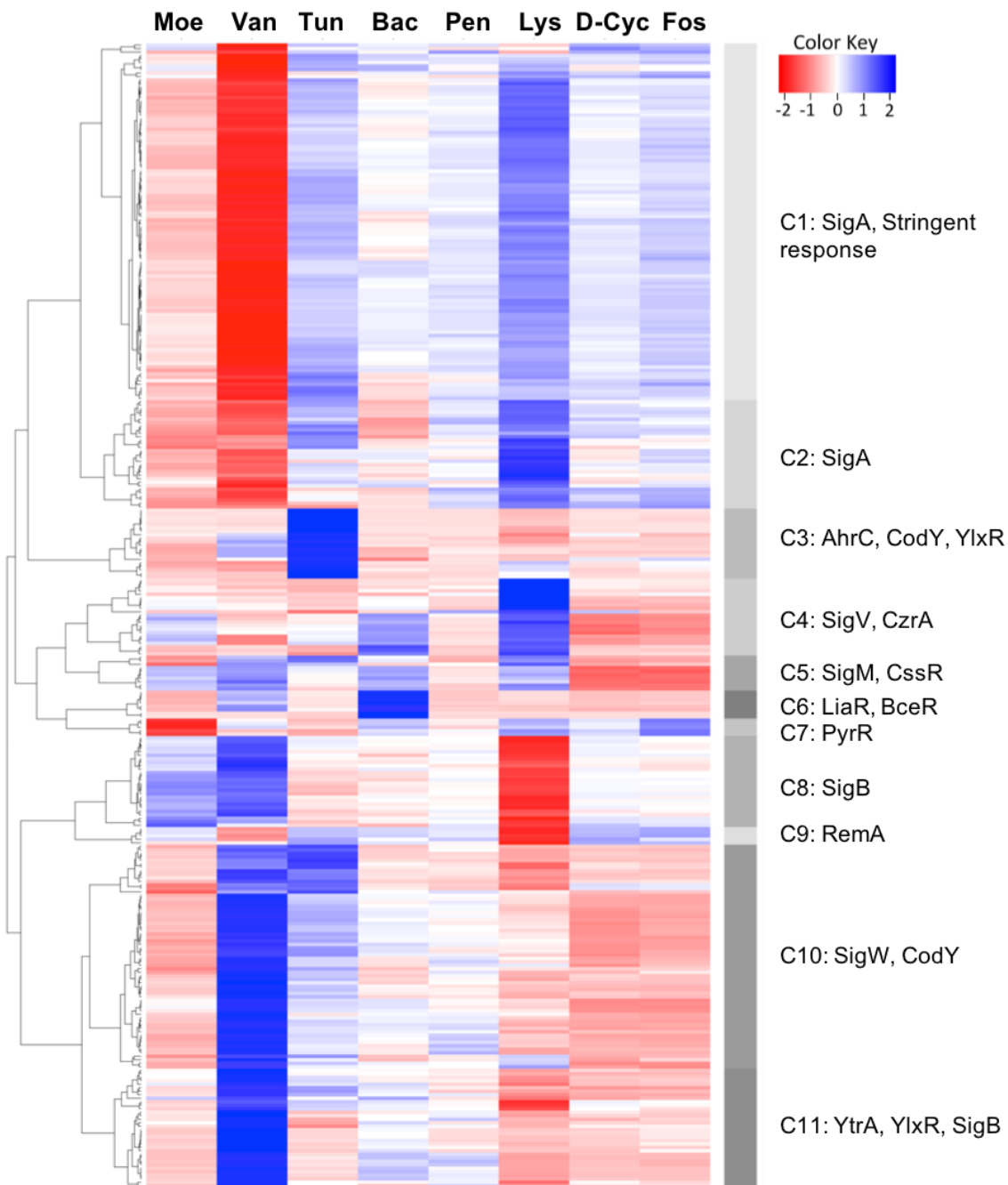


Fig. 2 Hierarchical clustering analysis of the transcriptional profiles of *B. subtilis* in response to cell envelope-active compounds (RNaseq). The heatmap was generated using “Heatmap.2” package in R program based on the log<sub>2</sub> fold-change of the 327 differentially expressed genes. Side bar marks the 11 Clusters generated during clustering analysis. The C in front of the numeral denotes “Cluster”, with the major regulons in that cluster displayed. Each column represents the corresponding stimulon as indicated on the top in three letters. Each row represents the expression of one gene across the stimulons. The Color Key square on the top left corner indicates that the highest gene expression level is colored in blue, while the lowest gene expression level is in red.

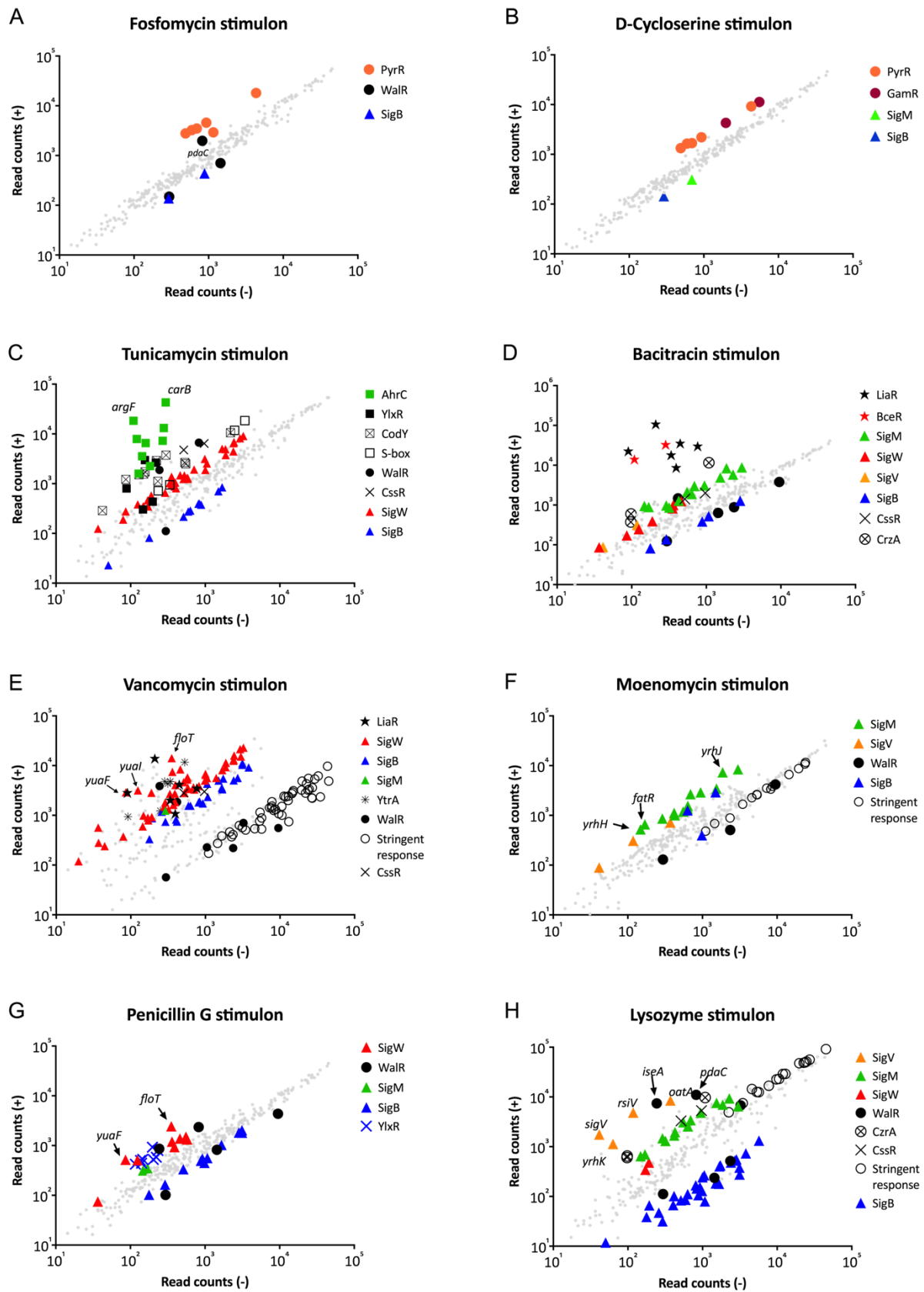


Fig. 3 Graphic presentation of the stimulons. Each graph represents the read counts of the genes in the treated sample (y-axis) against that in the untreated sample (wild type, x-axis). Most of the genes induced or repressed by at least 2-fold are highlighted using different symbols as indicated on the graph for each stimulon, with the corresponding regulators shown on the right side. Other genes are represented as smaller grey solid cycles. The read counts of each gene represent the mean value from the triplicates of each treatment.

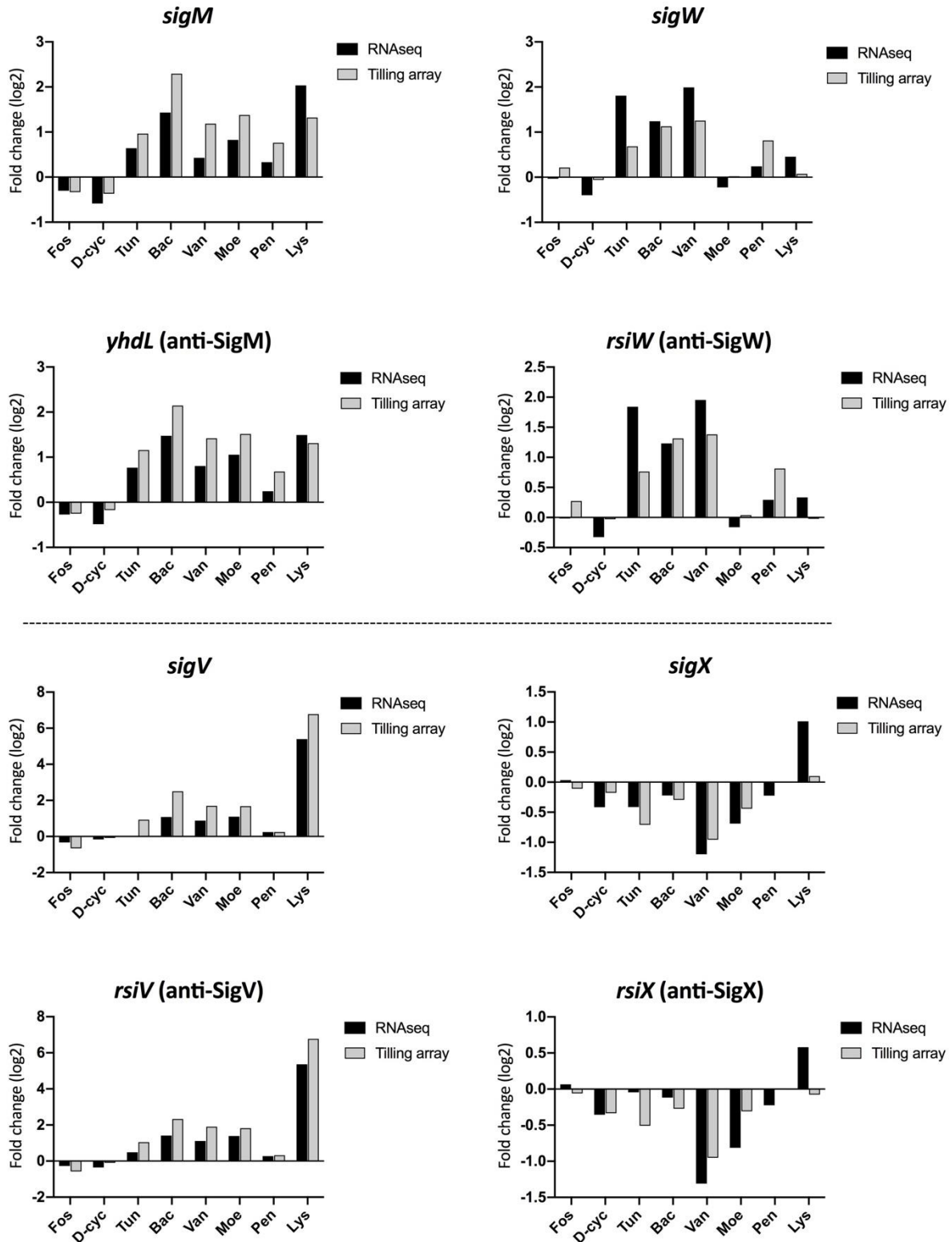


Fig. 4 Induction profiles of *sigW*, *sigM*, *sigV* and *sigX* by the CESs. The fold-change of each ECF  $\sigma$  factor represents the mean value from the triplicates of each treatment in RNAseq.

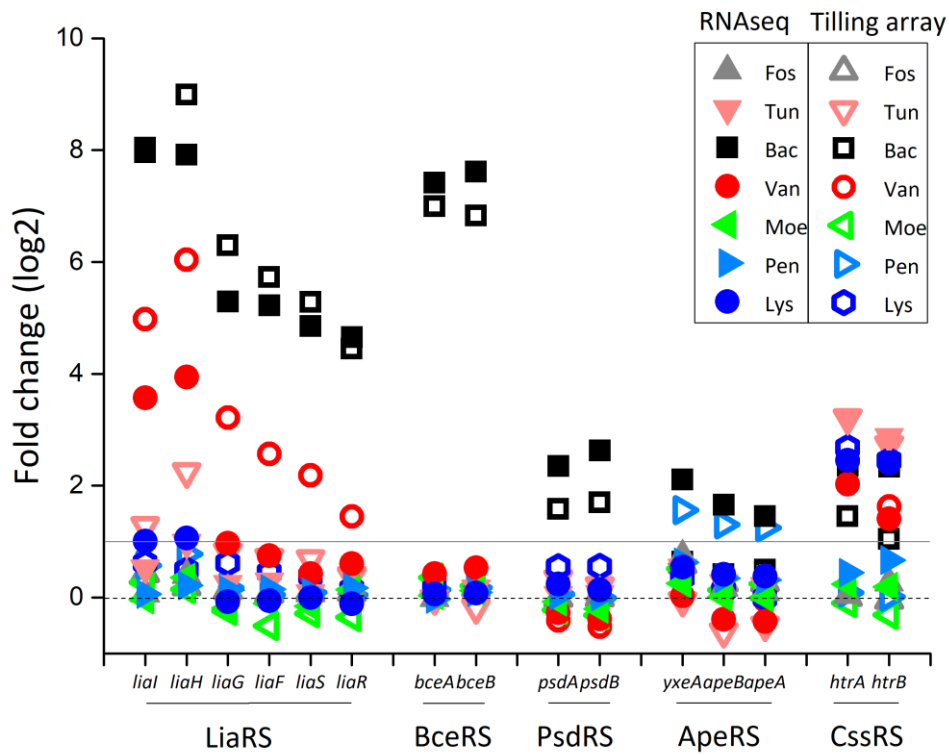


Fig. 5 Transcriptional response of two-component systems under cell envelope stresses. The operons regulated by the TCSs are indicated on the x-axis, with the corresponding TCS shown below. Each stack shows the DGE of each gene under different treatments, with the special conditions highlighted by distinct colors or symbols.

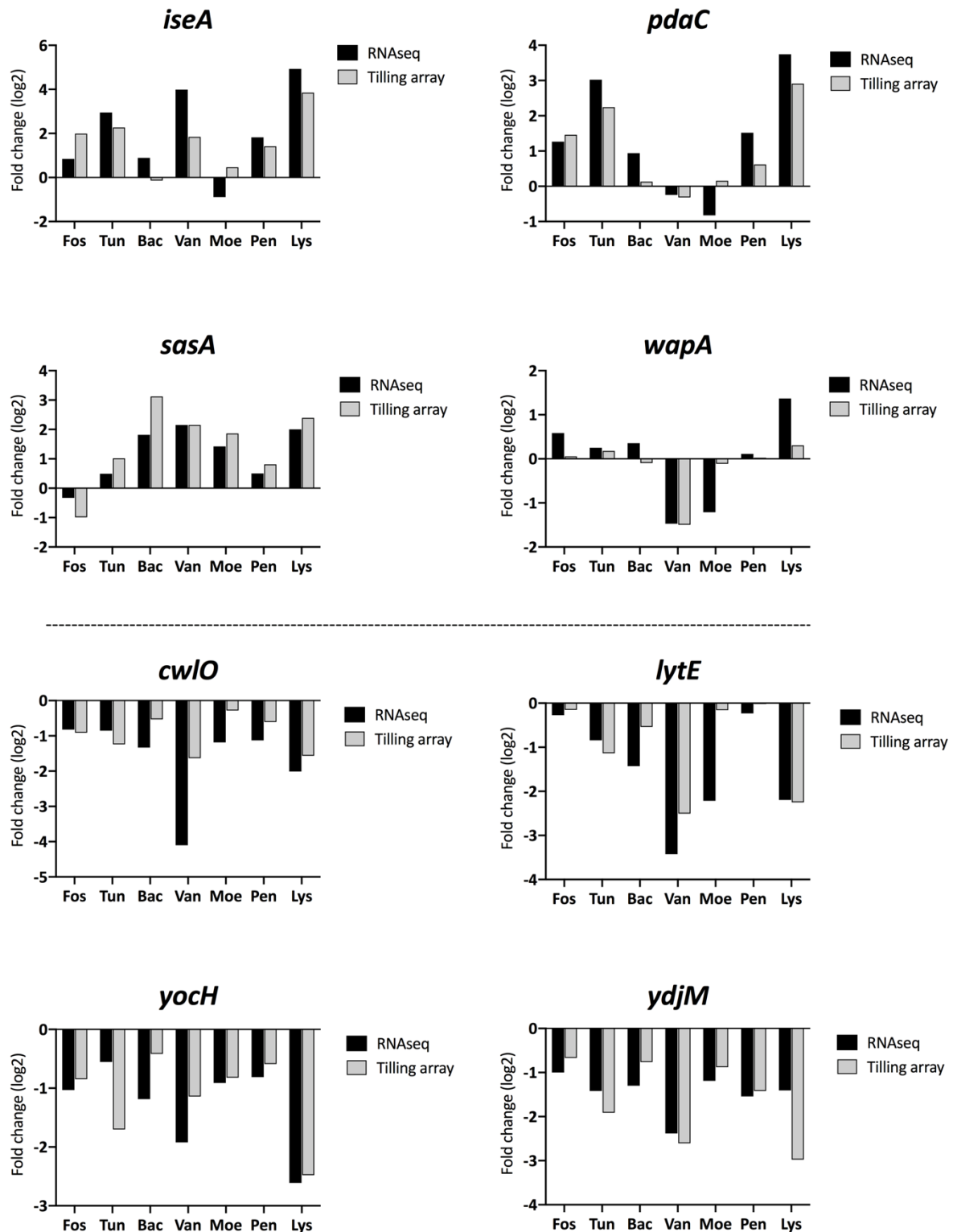


Fig. 6 Transcriptional response of WalR regulon to cell envelope-active compounds. The four graphs on the top half represent the induction profiles of the four genes repressed by WalR, and the four graphs below the dashed line represent the induction profiles of four of the genes activated by WalR.

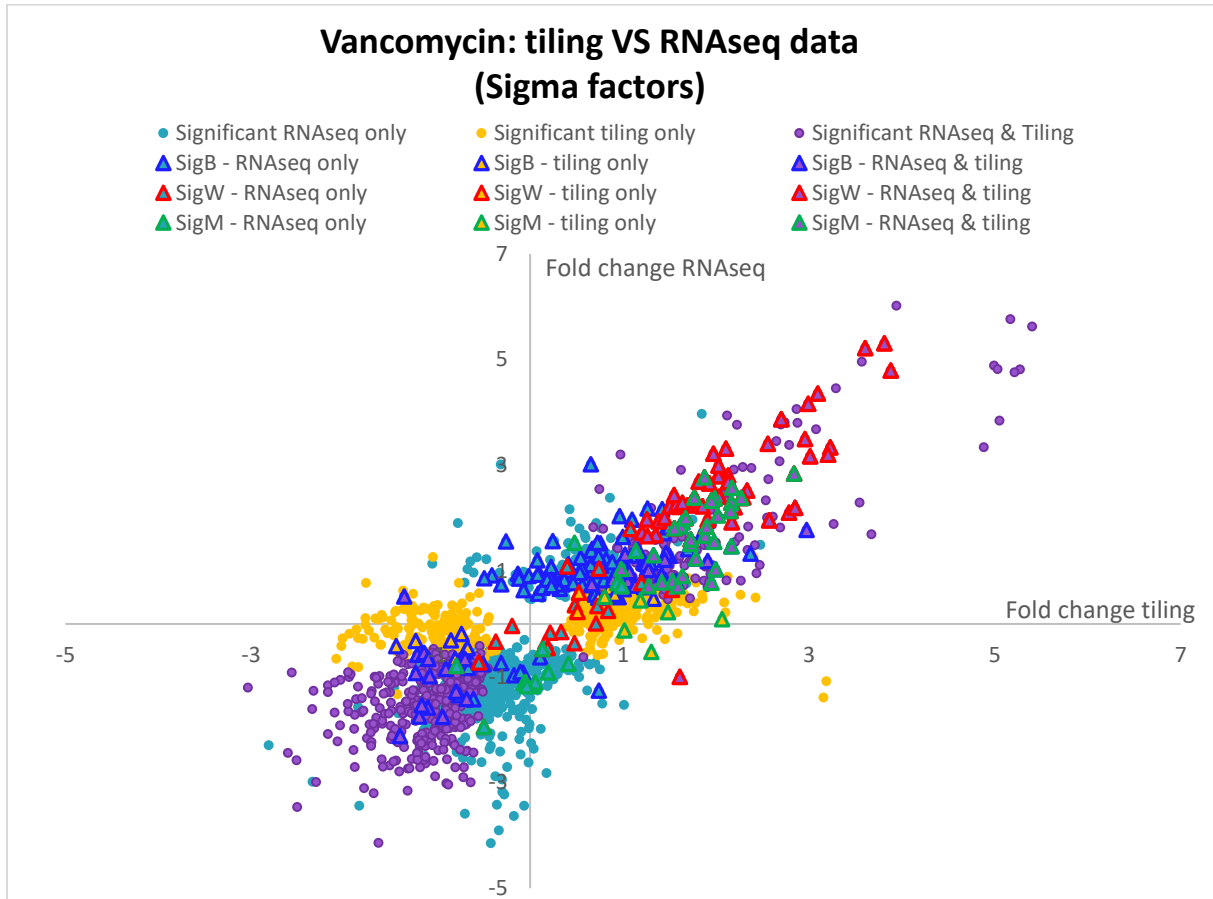


Fig. 7 vancomycin stimulon (RNAseq vs Tiling array)



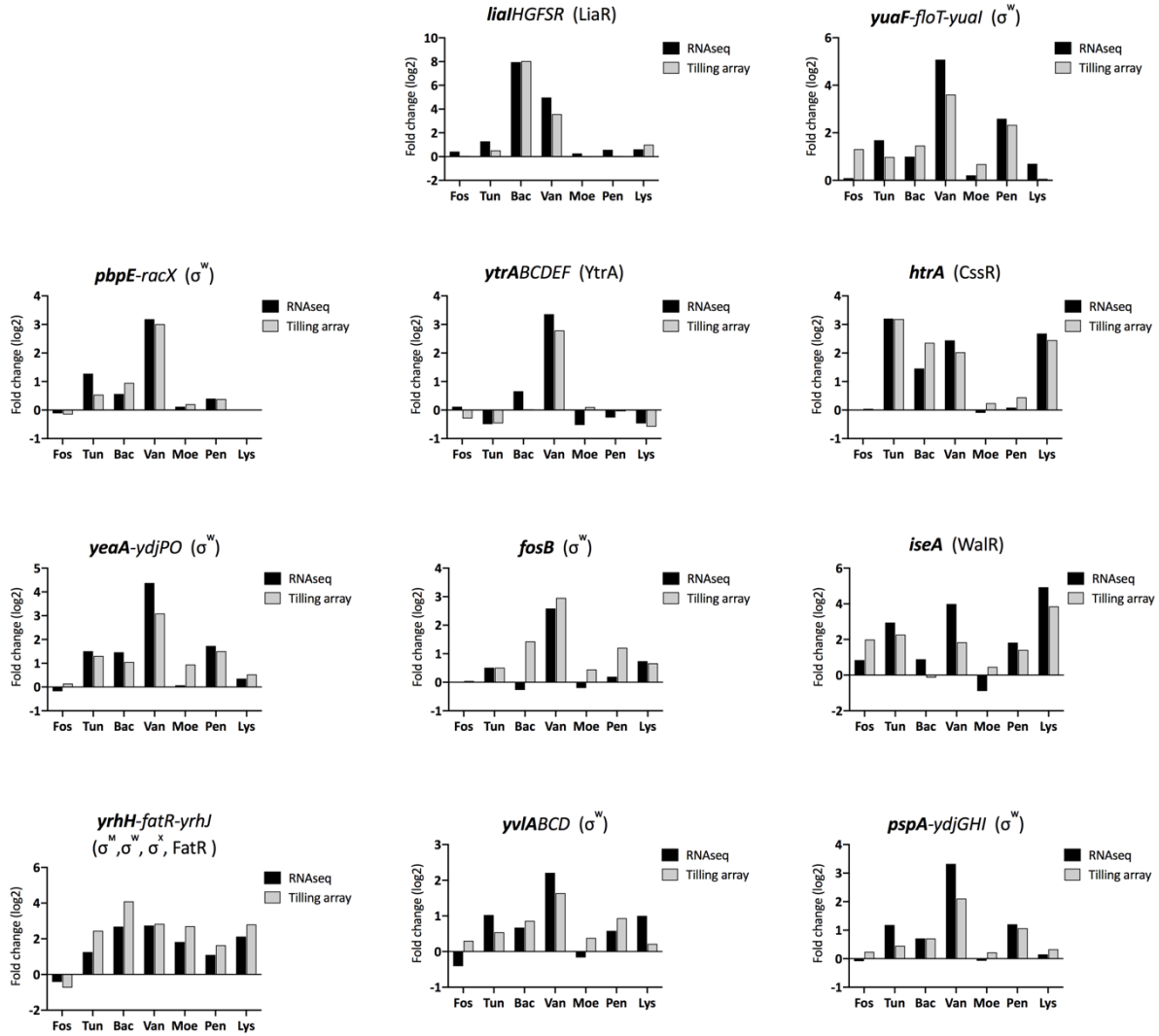


Fig. 8 Expression patterns of CCSR marker genes. In case of operons, the figure represents the induction profile of the gene of the operon marked in bold (usually the first gene of the operon). The corresponding regulator(s) for each gene or operon are displayed in parentheses.

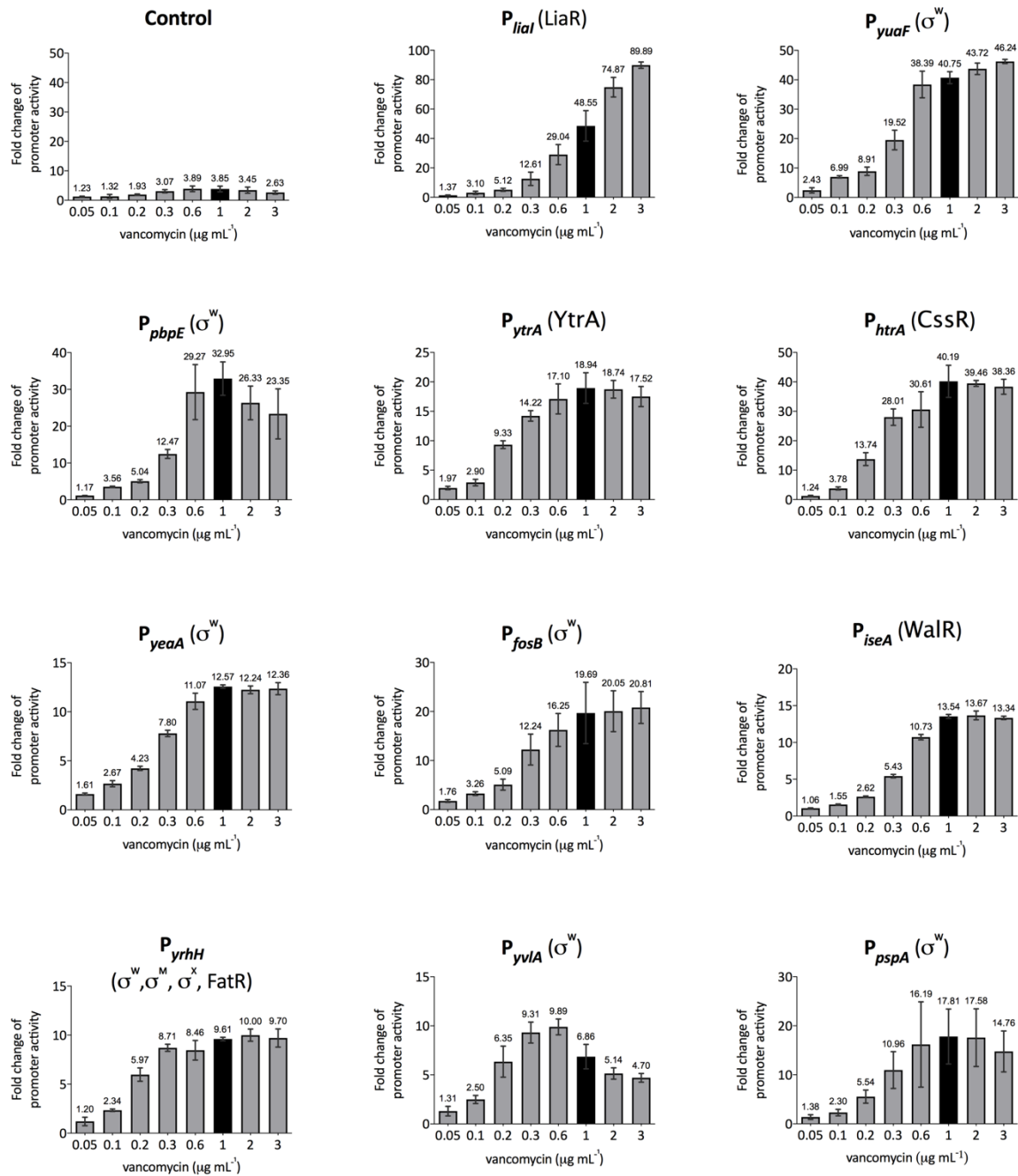


Fig. 9 Dose-dependent response of *B. subtilis* biosensors to vancomycin. The strain harboring promoterless-*lux* fusion was used as negative control. The biosensors after one hour of growth in a plate reader were treated with a series of concentrations of vancomycin, respectively, as indicated on the y-axis of each graph. The fold-change of promoter activity was obtained by normalizing the highest promoter activity, represented by luciferase activity (RLU/OD<sub>600</sub>, as shown in Fig.17 and Fig. S3), after the addition of vancomycin to the promoter activity under untreated condition (0  $\mu\text{g mL}^{-1}$ ) at the same time point. The promoter activities under 1  $\mu\text{g mL}^{-1}$  of vancomycin treatment are highlighted in black in order to compare with RNAseq data. Error bars indicate the standard deviation of at least three biological replicates.

## Supporting online material

### Comprehensive and Comparative Transcriptional Profiling of the Cell Wall Stress Response in *Bacillus subtilis*

Qian Zhang<sup>1#</sup>, Charlene Cornilleau<sup>2#</sup>, Raphael R. Müller<sup>3</sup>, Doreen Meier<sup>4</sup>, Pierre Flores<sup>2</sup>, Cyprien Guérin<sup>5</sup>, Diana Wolf<sup>1</sup>, Vincent Fromion<sup>2</sup>, Rut Carballido-Lopez<sup>2§</sup>,  
and Thorsten Mascher<sup>1§</sup>†

<sup>1</sup> Technische Universität (TU) Dresden, Institute of Microbiology, Germany

<sup>2</sup> MICALIS Institute, INRAE, AgroParisTech, Université Paris-Saclay, 78350 Jouy-en-Josas, France

<sup>3</sup> Bioinformatics and Systems Biology, Justus-Liebig-Universität, Gießen, Germany

<sup>4</sup> SYNMIKRO and Philipps-Universität Marburg, Germany

<sup>5</sup> MaIAGE, INRAE, Université Paris-Saclay, 78350 Jouy-en-Josas, France.

# These two authors contributed equally to this work

§ Authors for correspondence:

[thorsten.mascher@tu-dresden.de](mailto:thorsten.mascher@tu-dresden.de), [rut.carballido-lopez@inrae.fr](mailto:rut.carballido-lopez@inrae.fr)

#### Author contributions:

T.M and R.C.-L. conceived the study. Q.Z., C.C. and P.F. performed experiments. Q.Z. and C.C. analyzed the data and generated all figures and tables. C.G., D.M., R.R.M. and V.F. were involved in RNA isolation and/or analyzing the RNAseq and tiling array experiments. D.W. supervised the experimental work in the Mascher group. Q.Z. and T.M. wrote the original draft of the manuscript. All authors took part in the manuscript revision.

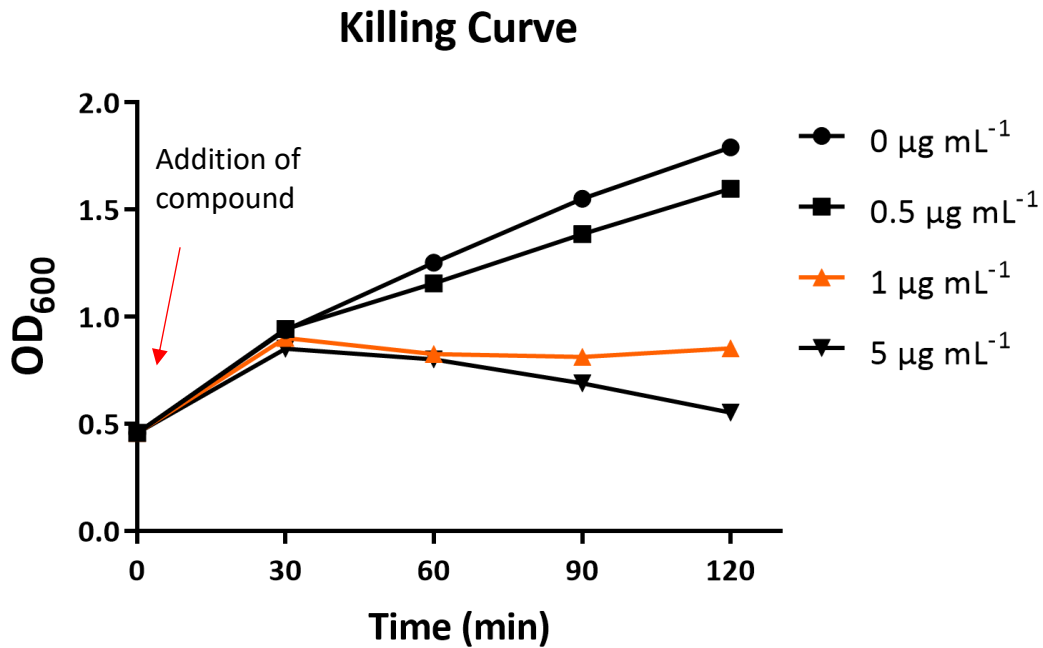


Fig. S1 Effect of treatment of different concentrations of vancomycin on *B. subtilis* growth. The killing curve assay results for vancomycin in RNAseq experiment was represented here to depict the definition of the sublethal concentration applied in this study. The sublethal concentration ( $1 \mu\text{g mL}^{-1}$ ) for vancomycin is highlighted in orange. The determination of the concentration for other compounds followed the same fashion.

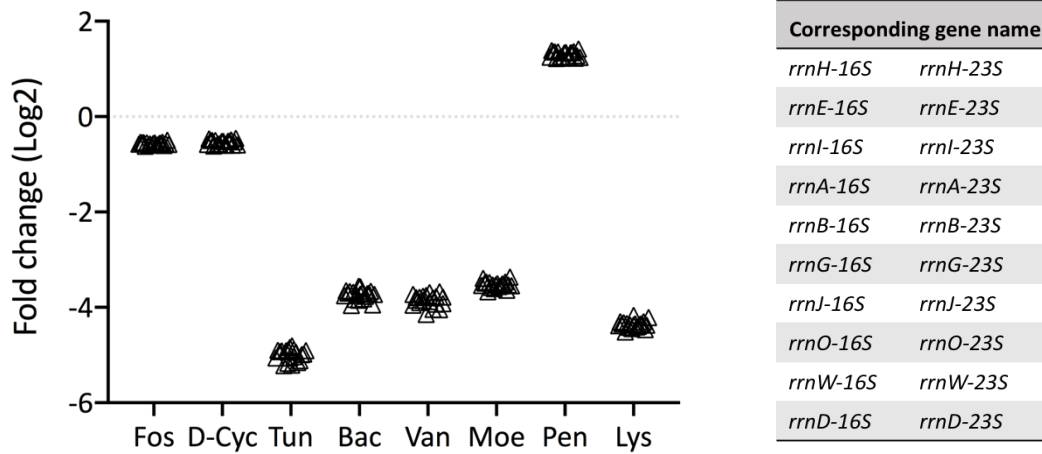


Fig. S2 Transcriptional response of rRNA-coding gene to different CEs. The 20 rRNA-coding genes are listed in the table on the right. The log2 fold change of these genes is displayed in the graph on the left with each gene represented by an open triangle. The triangles in each stimulon overlap because of their similar differential gene expression.

Fig. S3 Heatmap (tiling array)

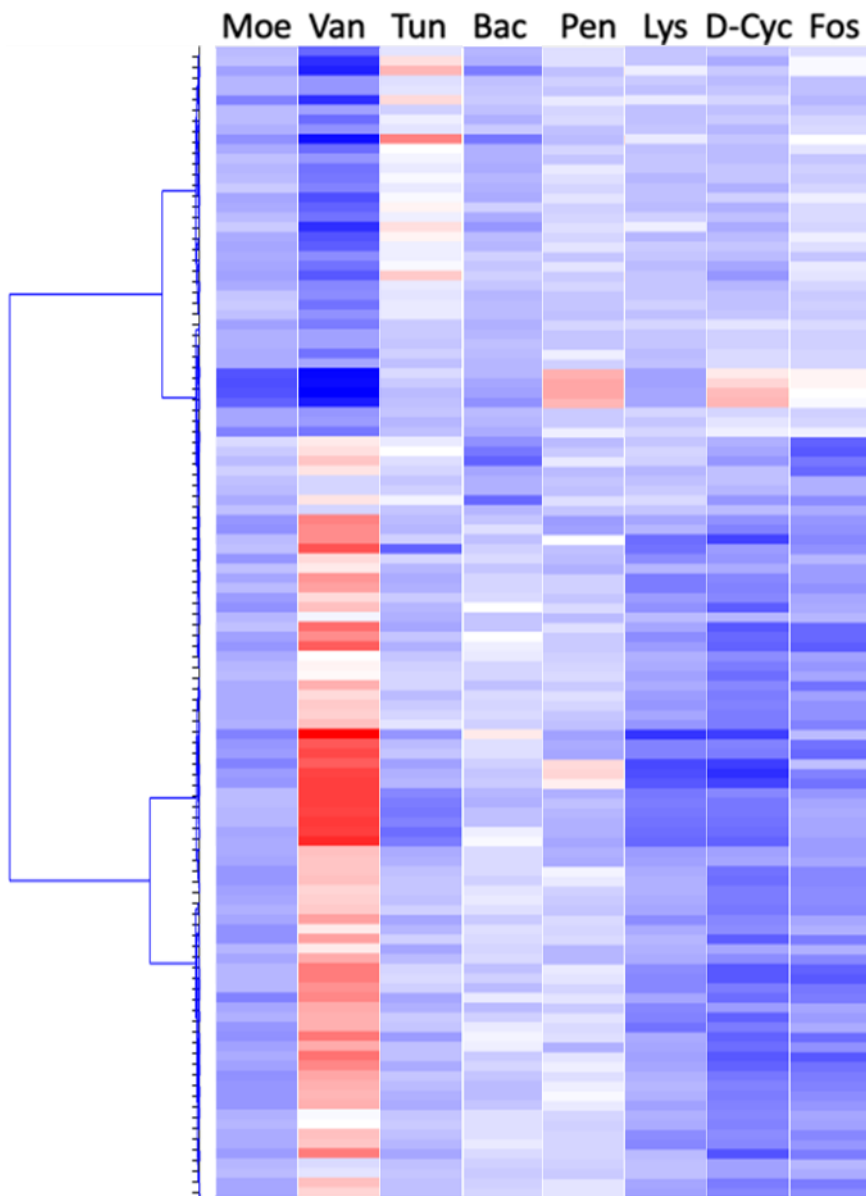


Fig. S3 Hierarchical clustering analysis of the transcriptional profiles of *B. subtilis* in response to cell envelope-active compounds (tiling array). Tiling array data in log<sub>2</sub> was used to generate the heatmap.

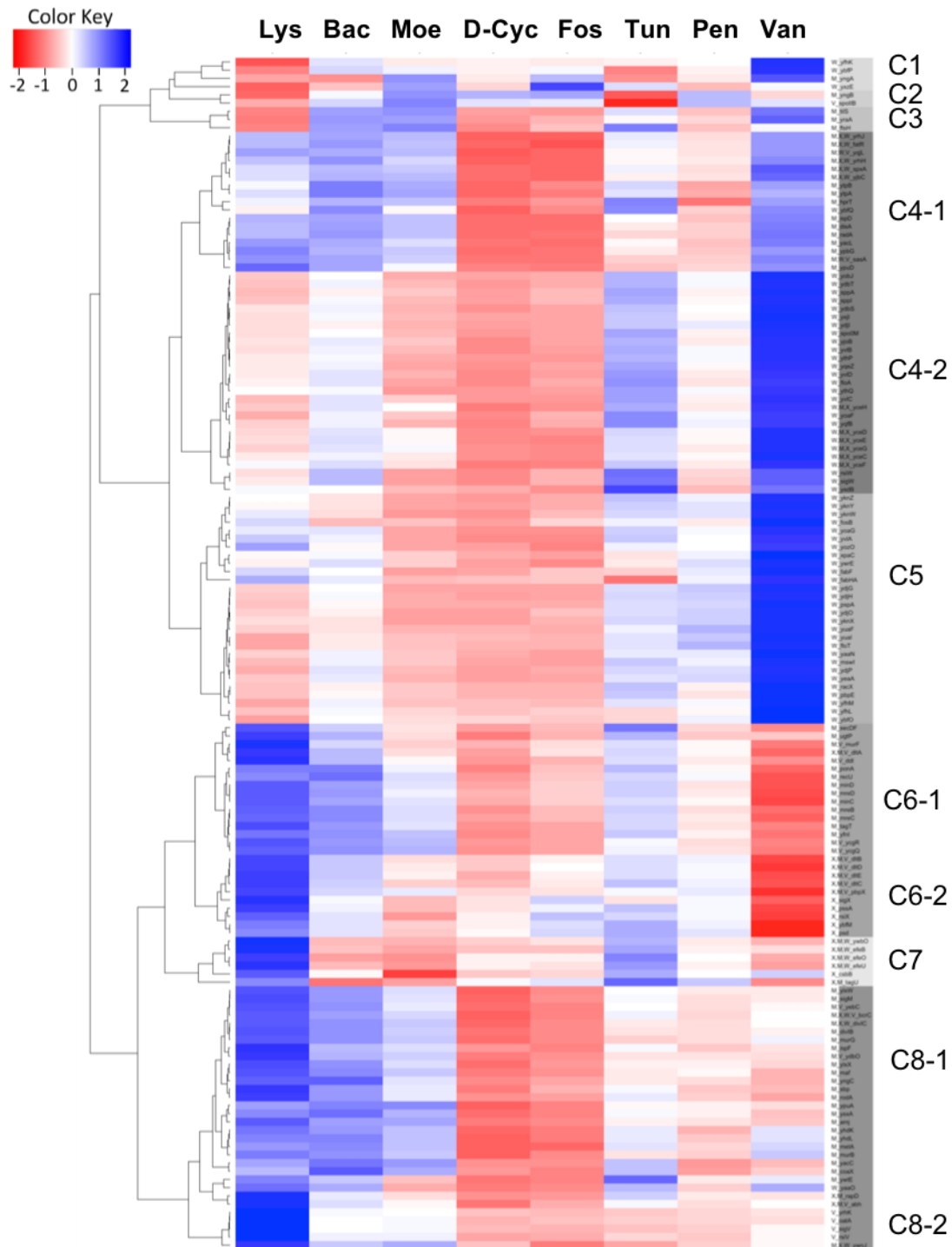
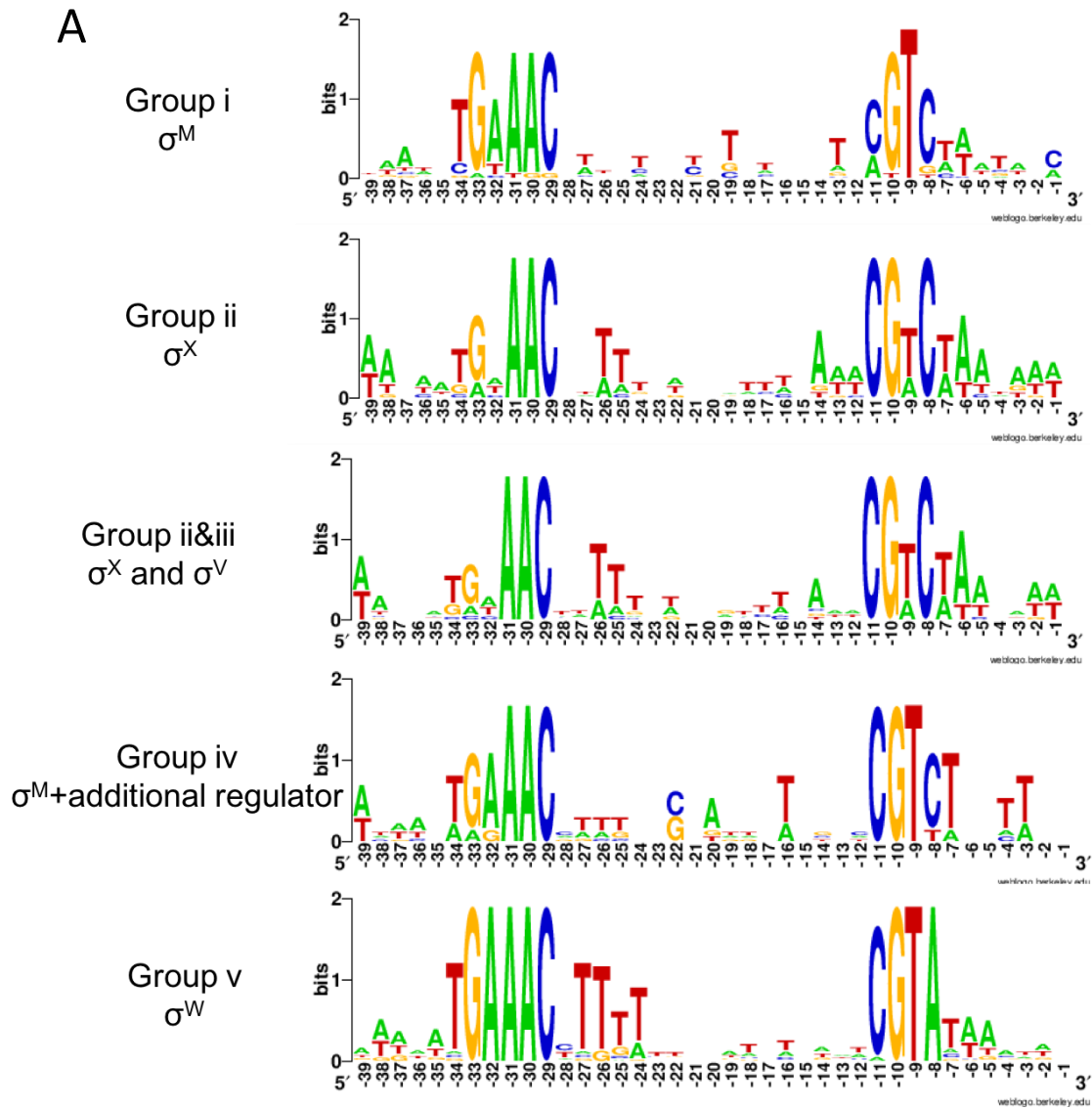
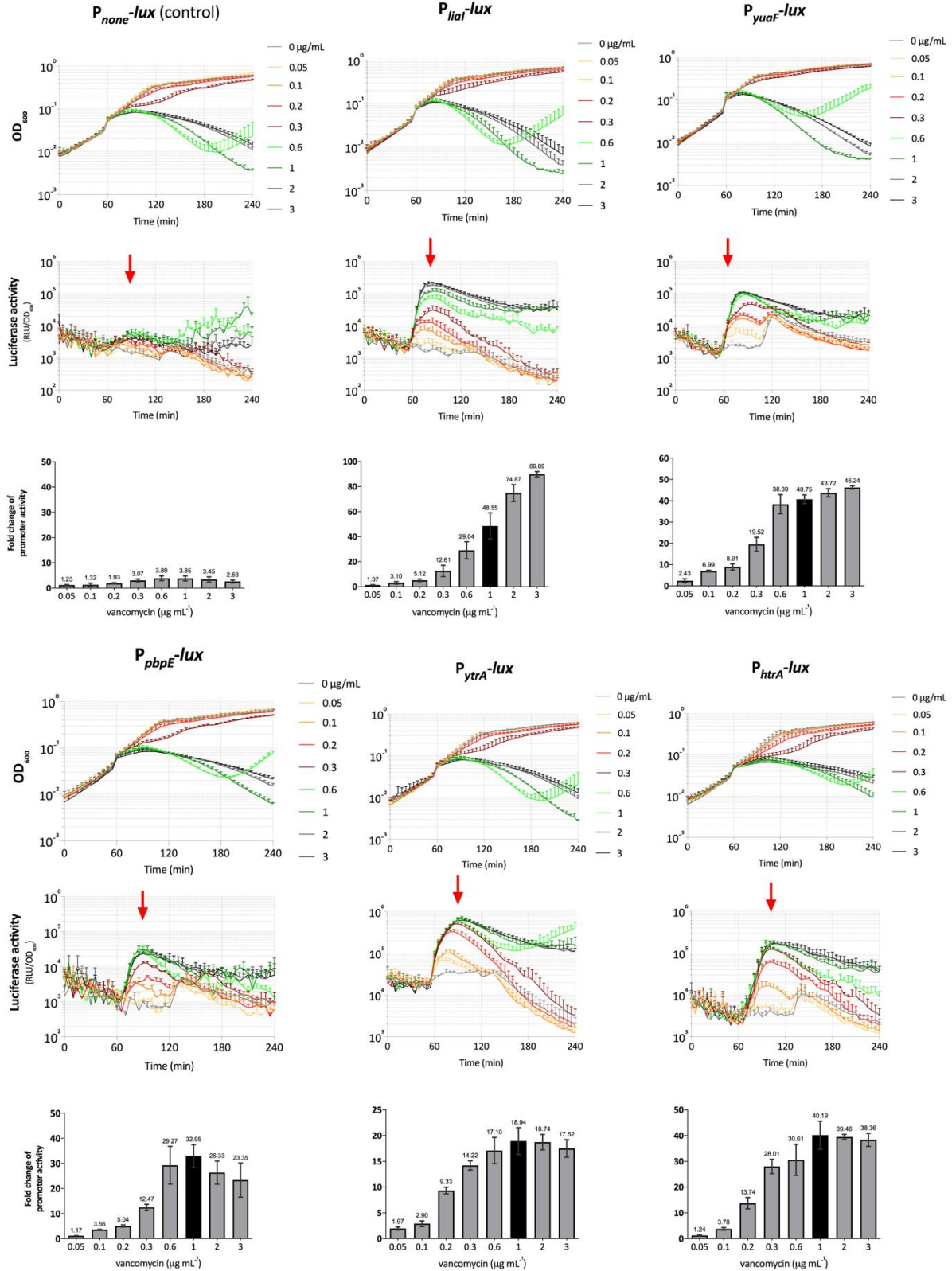


Fig. S4 Clustering analysis of the ECF sigma regulons. RNAseq data in log<sub>2</sub> was used to generate the heatmap. The RNAseq data applied here is the same as them in Table 1 in the main text which is shown with the data in fold change. The complete data for each gene of the ECF sigma regulons in each treatment conditions and their cluster assignment, shown as C1, C2 et al. at the side of the heatmap, is given in the table attached here.









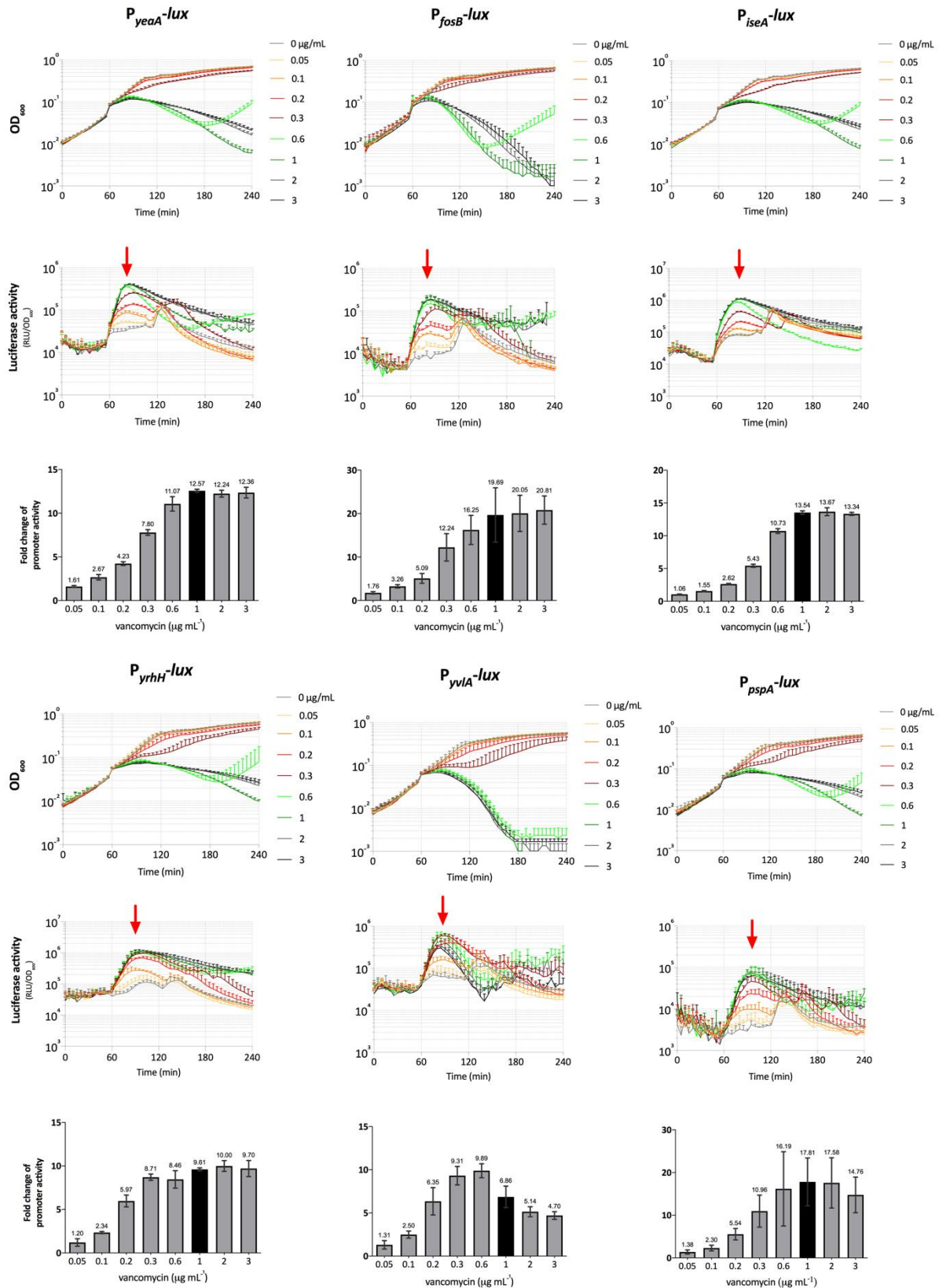


Fig. S6 Dose-response of *B. subtilis* biosensors to vancomycin.

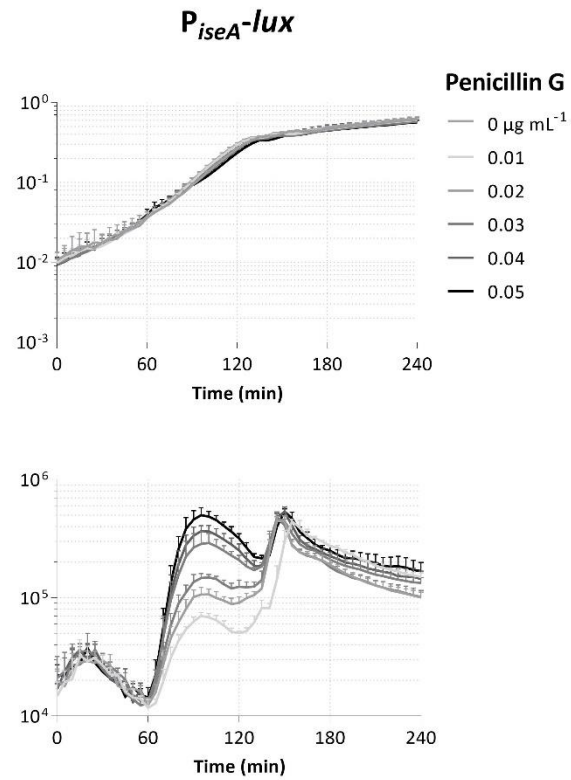


Fig. S7 Dose-response of *B. subtilis* biosensor with promoter  $P_{iseA}$  to penicillin G.

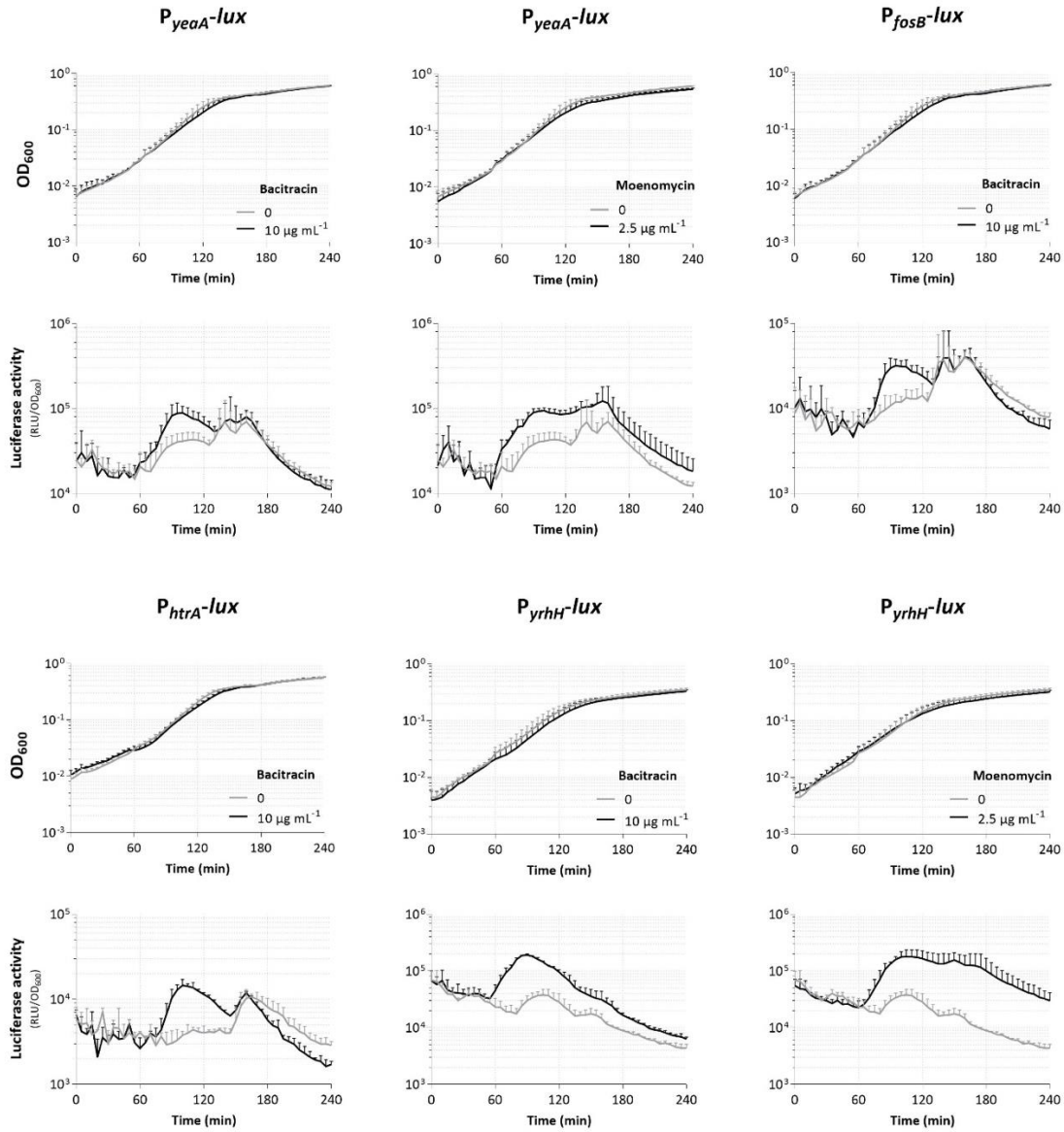


Fig. S8 Induction of *B. subtilis* biosensors to bacitracin and/or moenomycin.